Title: Transcriptional Landscape of Ectomycorrhizal Fungi and Their Host Provide Insight into N Uptake from Forest Soil

Running title: Transcriptional response of fungi and beech to N

Authors

Carmen Alicia Rivera Pérez[a#], Dennis Janz[a], Dominik Schneider[b], Rolf Daniel[b], Andrea Polle[a]

Affiliations

[a]Forest Botany and Tree Physiology, Büsgen Institute, Georg-August-University Göttingen, Büsgenweg 2, 37077 Göttingen, Germany

[b]Department of Genomic and Applied Microbiology and Göttingen Genomics Laboratory, Institute of Microbiology and Genetics, Georg-August-University Göttingen, Grisebachstrasse 8, 37077, Göttingen, Germany

[#]Correspondence: rivera@gwdg.de

Word count (abstract: 240/250; importance: 149/150; text: 4,862/5,000).

ABSTRACT Mineral nitrogen (N) is a major nutrient showing strong fluctuations in the environment due to anthropogenic activities. Acquisition and translocation of N to forest trees is achieved by highly diverse ectomycorrhizal fungi (EMF) living in symbioses with their host roots. Here, we examined colonized root tips to characterize the entire root-associated fungal community by DNA metabarcoding-Illumina sequencing of the fungal ITS2 molecular marker and used RNA sequencing to target metabolically active fungi and the plant transcriptome after N application. The study was conducted with beech (*Fagus sylvatica* L), a dominant tree species in central Europe, grown in native forest soil. We demonstrate strong enrichment of ^{15}N from nitrate or ammonium in the ectomycorrhizal roots by stable isotope labeling. The relative abundance of the EMF members in the fungal community was correlated with their transcriptional abundances. The fungal metatranscriptome covered KEGG and KOG categories similar to model fungi and did not reveal significant changes related to N metabolization but species-specific transcription patterns, supporting trait stability. In contrast to the resistance of the fungal metatranscriptome, the transcriptome of the host exhibited dedicated nitrate- or ammonium-responsive changes with upregulation of transporters and enzymes required for nitrate reduction and drastic enhancement of glutamine synthetase transcript levels, indicating channeling of ammonium into the pathway for plant protein biosynthesis. Our results support that self-composed fungal communities associated with tree roots buffer nutritional signals in their own metabolism but do not shield plants from high environmental N.

IMPORTANCE Although EMF are well known for their role in supporting tree N nutrition, the molecular mechanisms underlying N flux from the soil solution into the host through

the ectomycorrhizal pathway remain widely unknown. Furthermore, ammonium and nitrate availability in the soil solution is subject to constant oscillations that create a dynamic environment for the tree roots and associated microbes during N acquisition. Therefore, it is important to understand how root-associated mycobiomes and the tree roots handle these fluctuations. We studied the response of the symbiotic partners by screening their transcriptomes after a sudden environmental flux of nitrate or ammonium. We show that the fungi and the host respond asynchronously, with the fungi displaying resistance to increased nitrate or ammonium, and the host dynamically metabolizing the supplied N sources. This study provides insights into the molecular mechanisms of the symbiotic partners operating under N enrichment in a multidimensional symbiotic system.

KEYWORDS ammonium, *Fagus sylvatica*, fungi, metatranscriptome, mycorrhiza, nitrate, nitrogen stress, symbiosis

Soil N availability is generally a main limiting factor for primary productivity across terrestrial ecosystems including temperate forests (1, 2). In forest soil, soluble mineral N pools consist of nitrate and ammonium, whose quantities fluctuate in time and space, depending on soil properties, meteorological conditions, anthropogenic N inputs and biological processes such as mineralization, immobilization, and denitrification (3–12). While nitrate ions are highly mobile in soil solution and easily lost by leaching, ammonium cations are generally bound to soil colloids and retained in topsoil (13, 14). Consequently, mineral N nutrition of plants and microbes must cope with dynamic N availabilities in the environment.

The mutualistic association of certain soil EMF species with the root tips of forest trees is an ecological advantage to support nutrition of the host from variable environmental N sources (15–20). The vast majority of the root systems of individual trees in temperate forests are naturally colonized by a diverse spectrum of EMF species forming compound organs known as ectomycorrhizas and variably composed fungal communities (21–24). These ectomycorrhizas consist of root and fungal cells that mediate bidirectional nutrient exchange. EMF acquire N from the environment and transfer it to the root and receive host-derived carbon in return (25, 26). In self-assembled ectomycorrhizas, EMF show strong interspecific differences for N acquisition (27, 28). Early laboratory experiments showed that when the mycelium of EMF colonizing the roots of *Pinus sylvestris* and *Fagus sylvatica* was supplied with either ammonium or nitrate, the N sources became predominantly incorporated into the amino acids glutamate, glutamine, aspartate, asparagine and alanine (29, 30). When ammonium and nitrate were supplied at equimolar quantities to the mycelium of *Paxillus involutus*, ammonium incorporation into amino acids occurred in the fungus and nitrate remained almost unchanged, suggesting that EMF assimilate ammonium more readily than nitrate into amino acids prior to delivering it to the plant (31). Despite known discrimination between nitrate and ammonium (32, 33), most EMF have a widespread ability to metabolize nitrate (34, 35). Silencing the nitrate reductase (NR) gene in *Laccaria bicolor* impaired the formation of mycorrhizas with poplar (36) implying an important role of EMF in nitrate acquisition for the host.

The process of N transfer to the host through the mycorrhizal pathway starts at the soil-fungal interface, where different N forms are taken up from the soil solution by

fungal membrane transporters, N is then translocated through the fungal mantle, which wrapps the root tip, into the intraradical hyphae, and finally exported to the symbiotic interface becoming available for the plant (37–42). Studies on *Amanita muscaria*, *Hebeloma cylindrosporum*, *L. bicolor* and *Tuber melanosporum* have led to the hypotheses that ammonium is exported from the intraradical hyphae to the symbiotic interface through Ammonia/Ammonium Transport Out (Ato) proteins, voltage-dependent cation channels, and aquaporins (37, 43–46), and that amino acid export could occur through Acids Quinidine Resistance 1 proteins in *L. bicolor* and *H. cylindrosporum* (38, 44, 47). Moreover, the EMF-mediated import of ammonium and nitrate into the roots is supported by upregulation of ammonium transporters (43) and nitrate transporter (*NRT*) genes in ectomycorrhizal poplar roots like *PttNRT2.4A* with *A. muscaria* (48) and *PcNRT1.1 and PcNRT2.1* with *P. involutus* (49).

Once nitrate is taken up by NRTs, it is intracellularly reduced to nitrite by NR, then to ammonium by NiR and ammonium is ultimately incorporated into glutamine and glutamate (47, 50, 51). In the cyclic GS-GOGAT pathway, glutamine synthetase (GS) catalyzes the formation of glutamine by transfer of ammonium to glutamate. Then glutamate synthase (GOGAT) transfers the amino group from glutamine to 2-oxoglutarate generating two molecules of glutamate, whereas in the alternative pathway, the enzyme glutamate dehydrogenase (GDH) catalyzes the reductive amination of one molecule of 2-oxoglutarate using ammonium to generate one molecule of glutamate (50, 51). Both GS/GOGAT and GDH pathways operate in EMF but variations are common among species or symbiotic systems depending on the plant and fungal partners (52–54). In contrast to EMF, in plants the GS/GOGAT pathway

106 predominates and GDH plays a minor role in ammonium incorporation into organic N
107 forms (55). Currently, the molecular processes used by EMF for supplying mineral N to
108 the host in field conditions are unknown. Uncovering these molecular activities will
109 enable a better understanding of tree N nutrition and N cycling in the ecosystem.
110 Despite the well-recognized importance of the mycorrhizal pathway as a relevant
111 route whereby tree roots acquire N, knowledge of the molecular mechanisms operating
112 in the uptake, transport, and delivery of N to the host is limited to a few model EMF. It is
113 also unknown how EMF and the colonized root cells respond to variation in mineral N
114 availabilities. The "1000 Fungal Genomes Project" (56) along with the *Fagus sylvatica*
115 genome (57) provide a platform for disentangling fungal and plant transcriptional profiles
116 in self-assembled communities engaged in active symbioses. We took advantage of
117 new tools to unravel these responses in natural forest soil administering a N dose
118 corresponding to 29 kg N ha^{-1} yr^{-1}, a quantity in the range of an N saturated beech
119 forest (58, 59). To control N uptake and to distinguish responses to different N forms,
120 we fertilized with either ^{15}N-labeled ammonium or ^{15}N-labeled nitrate and then studied
121 transcriptional responses separately for EMF and the host trees using ectomycorrhizal
122 root tips (EMRTs). We used DNA-barcoding to describe the composition of the root-
123 associated fungal community and RNA sequencing to capture the metabolically active
124 fungi. We hypothesized that (i) the fungal community structure is unaffected after short-
125 term exposure to elevated N and that (ii) the transcriptional responses of metabolically
126 active EMF reveal molecular activities related to uptake and assimilation of nitrate and
127 ammonium. Since nitrate assimilation requires a series of reduction steps into
128 ammonium before its incorporation into amino acids, both distinct and overlapping

responses to nitrate and ammonium availability were expected to be imprinted in the transcription profiles of the symbiotic partners. Furthermore, we hypothesized that (iii) EMF buffer environmental fluctuations in N for the plant resulting in strong N-induced responses in the fungal metatranscriptome but only marginal effects in the root transcriptome, or alternatively that (iv) the entire symbiotic system forms a "holobiont" where the host and the EMF partners display synchronized and similar N-responses.

RESULTS

Abundance of root-associated fungal genera corresponds to transcriptional abundance. The global fungal community associated with beech roots in this experiment was dominated by six genera containing ectomycorrhizal (*Amanita:* 7.18%, *Cenococcum:* 9.05%, *Scleroderma:* 4.83%, *Xerocomus:* 29.17%), ericoid (*Oidiodendron:* 1.09%) and saprotrophic fungi (*Mycena:* 3.75%) (Fig. 1A; Data set 1). The remaining taxa were rare (< 1% per genus) and belonged to the phyla of Ascomycota (2.31%), Basidiomycota (2.51%), Mucoromycota (0.11%), Mortierellomycota (0.02%), and fungi of unknown phylogenetic lineage (39.98%) (Fig. 1A; Data set 1). We did not detect any significant effects of short-term ammonium or nitrate treatment on fungal OTU richness ($F_{2,9}$= 0.288, p= 0.756), on Shannon diversity ($F_{2,9}$= 0.437, p= 0.659) (Table S1), or on the composition of the fungal OTU assemblages (R^2= 0.146, pseudo-$F_{2,9}$= 0.767, p= 0.861, permutations = 9999, adonis, Fig. S1A).

Similarly as for the fungal OTUs, we aggregated the RNA counts of ectomycorrhizal fungi belonging the same genus (Fig. 1B). The transcript abundances obtained for individual genera were variable within replicates and treatment groups.

152 However, there were no significant differences among the fungal metatranscriptomes in
153 the nitrate, ammonium or control treatments (R^2= 0.198, pseudo-$F_{2,9}$= 1.110, p= 0.353,
154 permutations = 9999, adonis) (Fig. 1B; Fig. S1B). The transcript abundance of a specific
155 fungal genus was strongly correlated with the ITS-based abundance of that same genus
156 (R= 0.66, p< 0.001, Pearson, Fig. 1C), supporting that the metabolic activities of
157 abundant fungi associated with the beech roots were reflected. Fungi with low
158 abundances as determined by the DNA-based approach also showed significant
159 transcript abundances (Fig. 1C), implying that low-abundant fungi still may contribute
160 significantly to the molecular activities of the root mycobiome.

161 **Fungal metatranscriptomes cover fungal metabolism which hardly respond**
162 **to N treatments.** The RNA data containing ectomycorrhizal, ericoid mycorrhiza,
163 endophyte and saprotrophic fungi comprised a total of 175,531 transcript identifiers or
164 gene models, covering 3,759 unique Eukaryotic Orthologous Groups of protein
165 identifiers (KOGs). From these, 122,437 transcript ids (covering 3,708 unique KOGs)
166 belong purely to the EMF (Data set 2). After aggregating the fungi by KOGs into a
167 metatranscriptome and normalizing in DESeq2, the full list fungal metatranscriptome (17
168 fungi, see Table 1) resulted in 3,619 unique KOGs, whereas the EMF-specific
169 metatranscriptome (13 EMF species, see Table 1) comprised 3,593 KOGs (Data set 3).
170 We evaluated the molecular functions of the EMF metatranscriptome according to KOG
171 functional classifications. All 25 KOG functions were represented and categorized into
172 “cellular processing and signaling” (1,159 KOGs), “information, storage and processing”
173 (956 KOGs), “Metabolism” (796 KOGs), “poorly characterized” (817 KOGs), and
174 multiple function assignment (135 KOGs) (Fig. 2). The frequencies of these functional

175 classifications roughly reflected the same pattern of KOG frequencies present *in silico* in
176 the model EMF *L. bicolor* and that of *Laccaria* sp. on the beech roots (Fig. 2).
177 We further tested with DESeq2 whether the KOGs belonging to the full list fungal
178 metatranscriptome or only to the EMF metatranscriptome were significantly differentially
179 expressed in response to ammonium or nitrate treatment relative to the controls. In
180 response to ammonium, not a single KOG was significantly affected (Data set 3). In
181 response to nitrate, one differentially expressed KOG was detected (KOG4381) in the
182 full list fungal metatranscriptome and two KOGs (KOG4381 and KOG4431) in the EMF
183 metatranscriptome (Data set 3). KOG4381 (RUN domain-containing protein) was 578-
184 fold ($p_{adjusted}$ = 0.023943) and 550-fold ($p_{adjusted}$ = 0.020832) upregulated in the full list
185 and in the EMF metatranscriptomes, respectively (Data set 3). This KOG's function is
186 "signal transduction mechanisms" under the "cellular processes and signaling" category.
187 KOG4431 (uncharacterized protein induced by hypoxia) was 2.27-fold decreased
188 ($p_{ajusted}$ = 0.020832) in response to nitrate and has "poorly characterized function" (Data
189 set 3). Two fungi (*Cenococcum geophilum* and *Xerocomus badius*) occurred in all
190 samples (Fig. 1B), but because of overall low transcriptome coverage, we did not test
191 differential responses to N treatments for specific fungi.
192 Mapping the EMF metatranscriptome to the KEGG pathway database with *L.*
193 *bicolor* as reference revealed 108 metabolic pathways, including "biosynthesis of amino
194 acids," "carbon metabolism," and "nitrogen metabolism" (Table S2). From a total of 952
195 unique EC numbers, the complete (866) were mapped and the partial (86) were
196 excluded to avoid inaccurate multiple reaction assignments (60). KEGG pathway
197 enrichment analysis pooling all treatments revealed putative metabolic functions of the

EMF metatranscriptome with eleven significantly enriched pathways (FDR $P_{adjusted}$ <0.05), mainly for energy, carbon, amino acid and N metabolism: "glycolysis/glucogenesis," "pentose phosphate pathway," "pyruvate metabolism," "amino sugar and nucleotide sugar metabolism," "pyrimidine metabolism," "biosynthesis of amino acids," "arginine biosynthesis" (Table 2). While "nitrogen metabolism" was covered but not significant (P = 0.063) with the enzymes GS (EC 6.3.1.2), GDH (EC 1.4.1.2), nitrilase (EC 3.5.5.1), and carbonic anhydrase (EC 4.2.1.1). After manually searching the complete fungal transcriptional database (Data set 2), transcripts encoding proteins and enzymes for fungal N uptake and metabolism were discovered. These clustered according to the fungal species instead of putative transporter/enzyme function (Fig. 3). The samples did not clearly cluster according to treatments but formed two main clusters, one containing the majority of nitrate- and ammonium-treated samples (6/8), the controls (4/4), and 2 N-treated samples. However, these differences were not significant (R^2= 0.176, pseudo-$F_{2,9}$= 0.96161, p = 0.475, adonis).

^{15}N application records strong N uptake by roots with increased root N concentrations. The EMRTs showed a strong ^{15}N enrichment in response to $^{15}NH_4^+$ and $^{15}NO_3^-$ treatment (Table 3) although specific effects related to mineral N provision were not discovered in the EMF metatranscriptome. The ^{15}N enrichment in the root system decreased with increasing distance from the root tips and was about 2-times lower in fine roots, and about 6- to 8-times lower in coarse roots than in EMRTs (Table 3). The N content of the ^{15}N-treated roots was slightly and significantly increased in comparison to control roots (Table 3) supporting that short-term N application caused enhanced N uptake. Thus, the N treatments triggered a significant decrease in the fine

root C/N ratio compared to the controls (Table 3). The soil N content was not markedly affected by ^{15}N application and the ^{15}N signatures of nitrate- and ammonium-treated soils did not differ (Table 3). Overall, the beech root systems accumulated 1.5 ± 0.7% and 1.2 ± 0.6% of ^{15}N from ammonium or from nitrate, respectively (Table 3). Since assimilation of inorganic nitrogen requires carbon skeletons (51), we measured fine root non-structural carbohydrate concentrations. However, no significant effects of N treatment on the carbohydrate concentrations were detected (Table 3).

Beech transcriptome responds to nitrate and ammonium treatments activating N assimilation. Mapping of the RNA reads to the beech genome resulted in a total of 55,408 beech transcript ids or gene models before normalization (Data set 4) and 27,135 beech gene models after normalization (Data set 5) in DESEq2. Ammonium and nitrate treatment resulted in 75 and 74 differentially expressed beech gene models (DEGs), respectively, with both treatments sharing 26 DEGs (Fig. 4A) and indicating overlapping responses to ammonium and nitrate. Among these overlapping DEGs, a putative glutamine synthetase (*GS*, AT5G35630.2) showed the highest upregulation, along with five putative cysteine-rich receptor-like protein kinase orthologs of *Arabidopsis thaliana* (*CRK8*, AT4G23160.1), outward rectifying potassium channel protein (*ATKCO1*, AT5G55630.2), HXXXD-type acyl transferase family protein (AT5G67150.1), hemoglobin 1 (*HB1*, AT2G16060.1), molybdate transporter 1 (*MOT1*, AT2G25680.1), and early nodulin-like protein 20 (*ENODL20*, AT2G27035.1) (Fig. 4B). Moreover, among the downregulated overlapping DEGs were a cinnamate-4-hydroxylase (*C4H*, AT2G30490.1) which plays a role in plant phenylpropanoid metabolism, growth, and development (61), eight orthologs coding for a DNAse 1-like

superfamily protein (AT1G43760.1), AP2/B3-like transcription factor family proteins (*VRN1*, AT3G18990.1) which are involved in regulation of the vernalization pathway (62, 63), subtilase family protein (AT5G45650.1), Ankyrin repeat family protein (AT3G54070.1), LRR and NB-ARC domains-containing disease resistance protein (*LRRAC1*, AT3G14460.1) known to play roles in the immune response against biotrophic fungi and hemibiotrophic bacteria (64), and NB-ARC domain-containing disease resistance protein (AT4G27190.1) (Fig. 4B).

Among unique responses to ammonium treatment were upregulation of a further *GS* ortholog (AT5G35630.2) and downregulation of a putative nitrate transporter gene (*NRT1.5*, AT1G32450.1) (Fig. 4B) known to load nitrate into the xylem and to be induced at high or low nitrate concentration in *A. thaliana* (65). Among the unique DEGs detected in response to nitrate treatment and known to play roles in nitrate translocation and metabolism were a putative high affinity nitrate transporter (*NRT3.1*, AT5G50200.1) which was upregulated along with a putative nitrite transmembrane transporter (*ATNITR2;1*, AT5G62720.1, see (66), a nitrite reductase 1 (*NIR*, AT2G15620.1), a molybdate transporter 1 (*MOT1*, AT2G25680.1), a SLAC1 homologue 3 (*SLAH3*, AT5G24030.1), and chloride channel b (*CLC-B*, AT3G27170.1) genes (Fig. 4B). Furthermore, transcripts for the root-type ferredoxin:NADP(H) oxidoreductase gene (*RFNR1*, AT4G05390.1) which supplies electrons to Ferredoxin-dependent enzymes (e.g., Fd-NiR and Fd-GOGAT) (67), and a ferredoxin 3 gene (*FD3*, AT2G27510.1) which enables electron transfer activity were also upregulated, while a putative nitrate transporter gene (*NRT1/ PTR FAMILY 6.2*, AT2G26690.1) was down regulated (Fig. 4B). Other genes involved in N assimilation exhibited basal transcript levels, including

267 those coding for the enzymes GOGAT and GDH detected under nitrate, ammonium,
268 and control conditions but not differentially regulated.

269 Classification of beech DEGs into Mapman bins revealed a significant
270 overrepresentation of genes involved in “nitrogen metabolism” for both ammonium and
271 nitrate treatments (Fig. 5). Significantly overrepresented metabolic processes for the
272 nitrate treatment included “oxidative pentose phosphate pathway (OPP),” “protein,”
273 “redox,” “secondary metabolism,” “signaling” and “stress” (Fig. 5). For the ammonium
274 treatment, significantly overrepresented functions included “DNA,” “hormone
275 metabolism,” “secondary metabolism,” “signaling,” “stress” and “transport” (Fig. 5).
276 Pathway enrichment analysis of Gene Ontology terms of beech DEGs in g:Profiler
277 returned significant results for nitrate, but not for ammonium treatment. DEGs from the
278 nitrate treatment resulted in 38 significantly enriched GO terms involving nitrate-related
279 molecular level functions and four biological processes including “nitrate
280 transmembrane transporter activity,” “nitrite reductase activity,” “response to nitrate” and
281 “nitrate transport” (Table S3). Plant immune responses induced by nitrate were also
282 evident via the enrichment of a putative isochorismate synthase gene (*ICS2,*
283 AT1G18870) and a flavin-dependent monooxygenase 1 gene (*FMO1*, AT1G19250).
284 ICS2 is involved in the biosynthesis of vitamin K_1 (68) and potentially in salicylic acid
285 biosynthesis (69, 70). *FMO1* is involved in the catalytic conversion of pipecolic acid to
286 N-hydroxypipecolic acid (NHP) which plays a role in plant acquired systemic resistance
287 to infection by pathogens (71).

288 **DISCUSSION**

289 **Ectomycorrhizal and root acquisition of nitrate or ammonium**. A central aim
290 was to gain insights into gene regulation in self-assembled ectomycorrhizas by targeting
291 the transcriptomes of the fungi living in active symbiosis with beech roots in response to
292 N provision. To challenge fungal metabolism, we applied N treatments that caused
293 about 3- and 14-fold increases in the available NH_4^+-N (about 15.1 µg g^{-1} soil DW) and
294 NO_3^--N (about 2.3 µg g^{-1} soil DW), respectively. The magnitude of these variations was
295 similar to temporal fluctuations of NH_4^+-N and NO_3^--N observed in soil of beech stands
296 with 2-fold and 10-fold changes for NH_4^+-N and NO_3-N, respectively (72). Therefore, it
297 was expected to elicit representative N responses in the naturally assembled EMF
298 communities. The EMF assemblages in our study showed the typical patterns known for
299 temperate beech forests with high diversity (21, 23, 24), dominance of certain species
300 (73, 74) (e.g., genus *Amanita*, *Xerocomus* and *Scleroderma* in this study), and non-
301 uniform occurrence in the tree roots. However, the two-day N treatments were not
302 expected to affect the fungal community structure because colonization and
303 establishment of new ectomycorrhizas takes weeks or months rather than days (75, 76),
304 and shifts in fungal communities towards more nitrophilic fungi occur as a consequence
305 of long-term exposure to high N loads (77–81).
306 Our EMF community were composed of taxa characteristic for acidic sandy,
307 nutrient poor soils, including genera in the orders Agaricales, Boletales, Russulales,
308 Helotiales, Myltinidales and Thelephorales (Data set 1). These fungi vary in their
309 foraging strategies being equipped with different types of hyphae for scavenging N. *C.*
310 *geophilum* which is the most widespread fungus and known for its tolerance to drought
311 (82) produces short and medium-distance hyphae, while the hyphae of *Amanita*

(medium-distance smooth or long-distance), *Cortinarius* (medium-distance fringe), *Laccaria* and *Telephora* (medium-distance smooth), *Lactarius* (contact, short and medium distance), *Russula* (contact), and *Scleroderma* and *Xerocomus* (long-distance) are also diverse (78, 83). EMF that produce hydrophilic hyphae of contact, short, and medium-distance smooth exploration types were reported to respond positively or to display a mixed response to mineral N enrichment, whereas EMF with medium-distance fringe hydrophobic hyphae are the most sensitive, and those with long-distance hydrophobic hyphae vary in their responses to mineral N (78).

The availability of nitrate and ammonium ions in the soil of this experiment was made highly dynamic by a sudden increase. The high mobility of the negatively charged nitrate ions in the soil solution make it more available for the roots than the positively charged ammonium ions which tend to be fixed by soil colloids, and while both ions are prone to leaching in sandy soils, ammonium retention by organic matter and clay minerals is generally higher (5, 13, 14, 84). The lower energy cost needed for ammonium metabolism make its utilization more advantageous than nitrate. This was previously observed in EMF (30–35), and in agreement, we found higher translocation of ^{15}N from NH_4^+ than from NO_3^- to the coarse roots. Enrichment of the newly applied ^{15}N in the EMRTs was strong but did not differ between N form applied. We cannot exclude ammonification by soil microbes potentially converting NO_3^- to NH_4^+ in the soil before its uptake by the EMF, thus contributing to similar ^{15}N accumulation patterns in the ectomycorrhizas after NO_3^- or NH_4^+ application. Microbial turnover rates are estimated to be about 24 h for ammonium and a few days for nitrate (85). However, the significant transcriptional regulation of nitrate marker genes in beech roots under nitrate

exposure supports that NO_3^- was taken up by the root system. In fine root cells, NO_3^- was considerably more abundant than NH_4^+ as observed in beech trees in field conditions (72, 86) and unaffected by N addition. Our results demonstrate that the newly acquired ^{15}N was metabolized because the root N concentrations increased but not the levels of ammonium or nitrate.

N assimilation uncovers fungal taxon-specific but not N-induced transcription patterns in root associated fungal communities. Despite the compelling support for N uptake and assimilation in roots, the EMF metatranscriptome did not show any significant changes related to N metabolism. Initially, we hypothesized that if the root-associated fungi and the beech root cells responded like a synchronized "superorganism," both fungi and roots would show similar patterns in transcriptional regulation. However, this hypothesis is rejected because N-responsive DEGs were found in beech but not in the EMF metatranscriptomes, except for KOG4381 and KOG4431 which were induced by nitrate. Closer inspection revealed that KOG4381 occurred only in *Thelephora terrestris* and *Russula ochroleuca*, thus not reflecting a community response and rather suggesting that in the symbiotic system, the host and EMF partners respond as individual autonomous units. KOG4431 was present in nine EMF, including *Laccaria amethystina*, *Meliniomyces bicolor*, *Russula ochroleuca*, *Scleroderma citrinum*, *Thelephora terrestris*, *Xerocomus badius*, *Amanita rubescens*, *Boletus edulis* and *Cenococcum geophilum*. Further analyses are needed to clarify the role of these two KOGs in nitrate signaling. Although differentially expressed KOGs were limited in the fungal metatranscriptomes, putative transporters (NRT/NIT, AMT) and enzymes (NR, NiR, GS, GOGAT, and GDH) were transcribed (Fig.6), representing

all necessary steps for mineral N uptake and assimilation into amino acids. In controlled laboratory studies, many of these transporters and enzymes have been characterized in EMF and were regulated by N form and availability. For instance, high affinity nitrate/nitrite transporters (NRT2), nitrate reductase (NR) and nitrite reductase (NiR1) in *Hebeloma cylindrosporum* (87, 88), NRT2, NR1 and NiR1 in *Tuber borchii* (89, 90), NRT, NR and NiR in *L. bicolor* (44, 91), high and low affinity ammonium transporters (AMT1, AMT2, and AMT3) in *H. cylindrosporum* (50, 92), AMT2 in *Amanita muscaria* (93), and AMT1, AMT2 and AMT3 in *L. bicolor* (44). Although we did not find N-induced regulation of specific genes, GO term enrichment analysis shows that functions related to N assimilation and carbon metabolism were enriched across all studied EMF. We suggest that at the whole EMF community level, the primary metabolism is genetically equipped for handling fluctuating environmental N availability and host-derived C supply.

The observed stability of the fungal metatranscriptome was unexpected because stable isotope labeling and electrophysiological studies showed distinct responsiveness of different fungal taxa to environmental changes in self-assembled communities (27, 28, 94) and controlled studies (cited above and in the introduction) showed significant regulation of N-related genes. Our study does not exclude that there were N-induced responses in distinct fungi, but weak effects might have been masked by the variability of EMF species occurrence in individual cosms. Presumed species-specific responses to N fertilization were probably also overridden by inter-specific differences. This can be inferred from the observation that arrays of N-related genes clustered quite strictly according to species but not according to the genes with similar functions. Our

identification of expression patterns for the fungi under study is an important, novel result underpinning trait stability within naturally-assembled EMF in beech roots.

Ammonium and nitrate induce specific assimilation patterns in beech roots. Our initial hypothesis was that EMF shield the plant cells against major fluctuations in N availabilities and therefore we expected no or moderate changes in the beech root transcriptome after N fertilization. This hypothesis is rejected since both ammonium and nitrate treatments caused drastic changes in the beech root transcriptome. The strategy of European beech for dealing with high loads of inorganic N availability was transcriptional upregulation of genes involved in N uptake and assimilation, as observed in *Arabidopsis* (51),a non-mycorrhizal species. The transcription patterns in response to nitrate and ammonium were clearly distinguishable, in agreement with other studies that documented nitrate- and ammonium-specific effects on gene regulation, signaling and lateral root growth (95–100). Notably, transcripts belonging to putative NRTs and to enzymes (NR, NiR, GS) were significantly upregulated in the nitrate treatment encompassing the suite of reactions required for NO_3^- reduction and incorporation into amino acids (Fig. 6). In addition, upregulation of root ferredoxin and molybdate transporters pointed to an enhanced need for reducing power and the biosynthesis of NR, which requires molybdate in its active center (101). The significant activation of defenses against biotrophic fungi by nitrate was also remarkable. Similar results were shown in leaves of non-mycorrhizal nitrate-fed trees (102). In the ammonium treatment, significant upregulation of transcripts levels for two GS enzymes was detected, while a NRT1.5, potentially loading nitrate into the xylem, was downregulated. Remarkably, nitrate and ammonium treatments showed a common

pattern with strong upregulation of *GS* and *CRK*-like genes (Fig. 4B). CRK receptor kinases are involved in stress, plant pathogen response and cell death (103, 104). The *Arabidopsis* ortholog CRK8 is regulated in senescing leaves (105), and while a function in N metabolism appears likely, controlled experiments are needed. Overall, these results were in line with the expectation that nitrate-specific, ammonium-specific and overlapping responses were to be found. We demonstrate for the first time that excessive N in EMRTs is actively metabolized by the plant. It remains unknown if NO_3^- and NH_4^+ were taken up by EMF and transferred to the plant for further assimilation or if excessive N circumvented the fungal barrier, entering the plant directly (Fig. 6).

In conclusion, effects of high levels of ammonium or nitrate were not evident in the EMF metatranscriptome, whereas the host tree responded to ammonium and to nitrate by upregulating genes involved in assimilation of the surplus inorganic N into organic forms. Although it is unknown whether the applied ^{15}N sources underwent conversions due to microbial activities, the response of European beech indicated that a significant proportion of ammonium and nitrate was taken up in the originally added form. The fungal transcriptomes suggested species-specific N-metabolic responses, implying significant trait stability for N turnover and suggesting that EMF in temperate beech forests are resistant to short-term fluctuations in environmental N. However, further work is required to investigate to what extent this tolerant capacity can be sustained and its ecological relevance under chronic N exposure.

MATERIALS AND METHODS

Tree collection, maintenance, and experimental setup. European beech (*Fagus sylvatica* L.) saplings were collected on March 7th, 2018, in a 122-year-old beech

forest (53°07'27.7"N, 10°50'55.7"E, 101 m above sea level, Göhrde, Lower Saxony, Germany). The soil type is podzolic brown earth with parent material consisting of fluvio-glacial sands (106). In 2017, the mean annual temperature was 9.9 °C and the total annual precipitation 768 mm, whereas on the day of tree collection the mean air temperature was 4.6 °C and the precipitation was 0.66 mm (https://www.dwd.de). The beech saplings (n = 34) were excavated using polyvinyl chloride cylinders (diameter: 0.125 m, depth: 0.2 m), which were placed around a young tree, hammered into the ground to a depth of 0.2 m, and then carefully lifted to keep the root system in the intact forest soil. These experimental systems are referred to as cosms. The cosms were transported to the Forest Botanical Garden, University of Goettingen (51°33'27.1"N 9°57'30.2"E) where they were maintained outdoors under a transparent roof and exposed to natural climatic conditions except for rain (Table S4). A green shading net was placed over the roof to protect the trees from direct sun similar as in the forest. Thereby, on average, the full sun light was reduced on sunny days from 1125 µmol m^2 s^{-1} to 611 µmol m^{-2} s^{-1} PAR (photosynthetically active radiation) and on cloudy days from 284 µmol m^{-2} s^{-1} to 154 µmol m^{-2} s^{-1} (Quantum/Radiometer/Photometer model 185B, LI-COR Inc., Lincoln, NE, USA). The cosms were regularly watered with demineralized water. Control of the water quality (flow analyzer, SEAL AutoAnalyzer 3 HR, SEAL Analytical GmbH, Norderstedt, Germany) revealed 0.2 mg NH_4^+ L^{-1} and no detectable NO_3^- in the irrigation water. The cosms were randomly relocated every other day to avoid confounding positional effects. The trees were grown under these conditions until July 2018. By this time, the trees had a mean height of 0.401 ± 0.08 m

and a root collar diameter of 6.11 ± 0.95 mm. The trees were about 8 (± 2) years old based on the number of growth scars along the stem (107). Before the ^{15}N treatments, ammonium and nitrate were measured in the soil (details in Text S1). The cosms contained 15.1 ± 11.3 µg NH_4^+-N g^{-1} soil DW and 2.3 ± 1.3 µg NO_3^--N g^{-1} soil DW (n = 3, ±SD), equivalent to approximately 9.1 mg NH_4^+-N and 1.8 mg NO_3^--N $cosm^{-1}$.

Application of ^{15}N-labelled ammonium and nitrate. Before labeling, even distribution of irrigation solution in the soil was tested on separate cosms using blue dye ("GEKO" Lebensmittelfarbe, Wolfram Medenbach, Gotha, Germany) in water. The experimental cosms were assigned the following treatments: control (no nitrogen application), $^{15}NH_4^+$ application or $^{15}NO_3^-$ application. The cosms were surface-irrigated at 7 am with 60 ml of either 19.85 mM $^{15}NH_4Cl$ (99% ^{15}N, Cambridge Isotope Laboratories, Inc., MA, US, pH 5.47) or a 19.98 mM $^{15}KNO_3$ (99% ^{15}N, Cambridge Isotope Laboratories, pH 6.23) solution prepared in autoclaved deionized water. Controls were irrigated with 60 ml autoclaved demineralized water (pH 6.07). Each of these treatments were repeated the next day, resulting in a total application of 35.96 mg ^{15}N in the nitrate treated cosms or 35.74 mg ^{15}N in the ammonium treated cosms, corresponding to mean additions of approximately 30 µg ^{15}N g^{-1} dry soil. Treatments were conducted in two batches: batch 1: ^{15}N application on July 17th, 2018 and harvest on July 19th, 2018, n = 9 cosms; batch 2: ^{15}N application on July 31st, 2018 and harvest on August 2nd, 2018, n = 16 cosms.

Cosm harvest. The cosms were harvested 48 h after initial ^{15}N application. The tree-soil compartment was pushed out of the cylinder, collecting all parts. Roots were briefly rinsed with tap water, then with deionized water, and gently surface-dried with

paper towels. The root tips were clipped off, shock-frozen in liquid nitrogen, and stored at -80°C. Aliquots of fine roots were shock-frozen in liquid nitrogen and stored at -80°C and -20°C and soil aliquots at -20°C. During the harvests, the fresh masses of all fractions (leaves, stem, coarse roots, fine roots, root tips and soil) were recorded and aliquots were taken for dry-to-fresh mass determination after drying at 40°C (leaves, stems, soil) or after freeze-drying (coarse roots, fine roots and root tips). Biomass and soil mass in the cosms were calculated:

$$Total\ dry\ mass\ (g) = \frac{total\ fresh\ weight\ x\ aliquot\ dry\ weight}{aliquot\ fresh\ weight}$$

Soil and root chemistry. Soil pH was measured with a WTW pH meter 538 (WTW, Weilheim, Germany) using a ratio of dry sieved soil to water of 1: 2.5 according to the Forestry Analytics manual (108), A3.1.1.1, page 2. The water content in the soil was calculated as:

$$Relative\ soil\ water\ content\ (\%) = \frac{fresh\ soil\ weight - \ dry\ soil\ weight}{dry\ soil\ weight} x\ 100$$

For ^{15}N analyses, freeze-dried aliquots of soil, root tips, fine and coarse roots were milled using a ball mill (Type MM400, Retsch GmbH, Haan, Germany) in stainless steel grinding jars at a frequency of 30/sec in 20 second intervals to avoid heating the sample. The powder (control samples: 1.5 to 2 mg plant tissues, 5 mg soil; labeled samples: 1.5 to 3 mg plant tissue, 5 to 13 mg soil) was weighed into tin capsules (IVA Analysentechnik GmbH & Co KG, Meerbusch, Germany) and measured at the KOSI (Kompetenzzentrum Stabile Isotope, Göttingen, Germany). The ^{15}N samples were measured in the isotope mass spectrometer (Delta V Advantage, Thermo Electron,

493 Bremen Germany) and an elemental analyzer (Flash 2000, Thermo Fisher Scientific,
494 Cambridge, UK) and the non-labeled control samples in a mass spectrometer: Delta
495 plus, Finnigan MAT, Bremen, Germany and elemental analyzer: NA1110, CE-
496 Instruments, Rodano, Milano, Italy). Acetanilide (10.36 % N, 71.09 % C, Merck KGaA,
497 Darmstadt, Germany) was used as the standard. Enrichments of ^{15}N in the
498 ectomycorrhizal root tips (EMRTs), fine roots, coarse roots and soil were calculated as:

499 $$^{15}N\ enrichment\ (mg\ g^{-1}DW) = \frac{APE}{100}\ x\ Nconcentration\ of\ the\ sample\ (g\ g^{-1}DW)\ x\ 1000$$

500 where

501 $APE\ (atom\ \%\ excess) = atom\ \%\ ^{15}N_{labelled\ sample} - atom\ \%\ ^{15}N_{non-labelle\ \ sample}$ and

502 $atom\ \%\ ^{15}N = (^{15}N)/(^{14}N + {}^{15}N)\ x\ 100$

503 For determination of NH_4^+, NO_3^- and non-structural carbohydrates, frozen fine
504 roots (-80°C) were milled (MM400, Retsch GmbH) under liquid nitrogen to avoid
505 thawing. For mineral N determination, the frozen powder (approximately 55 mg per test)
506 were extracted as described before (109) with slight modifications and measured
507 spectrophotometrically with the Spectroquant® (1.09713.0002) Nitrate and Ammonium
508 (1.14752.0002) Test Kits (Merk, KGaA, Darmstadt, Germany). Glucose, fructose,
509 sucrose and starch were extracted from approximately 75 mg root powder and were
510 measured enzymatically as described before (110). Details of all procedures are
511 reported in (Text S1).

512 **DNA extraction, Illumina sequencing, bioinformatic processing and data**
513 **analyses of fungi.** Root tips (from -80°C) were homogenized in liquid nitrogen using
514 sterilized mortar and pestle. Each powdered, frozen sample was split in two parts: one

for DNA extraction and Illumina sequencing of the fungal ITS2 gene and the other for RNA extraction and mRNA sequencing. DNA was extracted from approximately 200 mg powder of root tips using the innuPREP Plant DNA Kit (Analytik Jena, AG, Jena, Germany). Extraction, purification, processing and sequencing are described in detail (Text S1). Briefly, the fungal nuclear ribosomal DNA internal transcribed spacer (ITS2) region was amplified by Polymerase Chain Reaction (PCR) using the primer pair ITS3_KYO2 (111) and ITS4 (112), both containing specific Illumina overhang adapters (in italics, primers underlined): forward (Miseq_ITS3_KYO2): 5'-*TCGTCGGCAGCGTCAGATGTGTATAAGAGACAG*GATGAAGAACGYAGYRAA-3'; reverse (Miseq_ITS4): 5'-*GTCTCGTGGGCTCGGAGATGTGTATAAGAGACAG*TCCTCCGCTTATTGATATGC-3'

After the PCR, the amplicons were purified and sequenced on a MiSeq flow cell using Reagent Kit v3 and 2x300 pair-end reads (Illumina Inc., San Diego, USA) according to the manufacturer's instructions at the Göttingen Genomics Laboratory (G2L, Institute of Microbiology and Genetics, Georg-August-University Göttingen, Göttingen, Germany). The raw sequences were quality filtered and clustered according to amplicon sequence variants (ASVs) at 97% sequence identity (i.e., operation taxonomic units, OTUs). Fungal reads were mapped to operational taxonomic units (OTUs) and abundance tables were generated. Taxonomic assignment of OTUs was carried out against the UNITE database v8.2 (04.02.2020),(113). All unidentified ASVs were searched (blastn) (114) against the nt database (2020-01-17) to remove non-fungal ASVs. Extrinsic domain ASVs and unclassified ASVs were discarded from the taxonomic table. The

538 fungal OTUs were assigned to trophic modes using the FUNGuild annotation tool (115).
539 The sequencing depth per sample was controlled by rarefaction analysis using the
540 package ampvis2 (116) and the samples were normalized by rarefying to the sample
541 with the lowest sequencing depth (i.e. 20,051 sequence reads). An overview of the
542 sequence processing results is provided in Table S5, and the rarefied abundance table
543 with taxonomic and guild assignment of OTUs is provided in (Data set 1).

544 **RNA extraction, library preparation, sequencing, and bioinformatic**
545 **processing of the fungal metatranscriptome and beech transcriptome.** Total RNA
546 was isolated from the frozen powder of beech root tips using a CTAB method (117). The
547 details have been reported in (Text S1). RNA integrity numbers (RIN), library
548 preparation and sequencing were conducted at Chronix Biomedical GmbH (Goettingen,
549 Germany). Twelve samples with RIN ranging from 6.7 to 7.9 were selected for polyA
550 mRNA library preparation (Table S6). Libraries were constructed with the NEBNext
551 RNA Ultra II Library Prep Kit for Illumina (New England Biolabs, Ipswich,
552 Massachusetts, United States) from 1 µg of purified RNA according to the
553 manufacturer's instructions. Single-end reads with a length of 75 bp were sequenced on
554 a NextSeq 500 Sequencing System instrument (Illumina, San Diego, CA, USA) with a
555 sequencing depth of 100 million reads per sample.

556 Processing (trimming, quality filtering and adapter removal) of the raw sequence
557 data (ca. 110 million reads per sample) resulted in approximately 109 million reads per
558 sample (Table S6). The reads were mapped against the reference transcriptomes of
559 *Fagus sylvatica* and 17 fungal species belonging to the same genera as those detected
560 by ITS barcoding (Table 1). Reference beech sequences and annotations were

561 downloaded from beechgenome.net (57) and reference fungal sequences and
562 annotations were downloaded from the JGI MycoCosm database (56). The resulting 18
563 fasta files were concatenated to one single file, which was used to create an index file
564 with bowtie2-build (118). The reads were mapped against this index file using bowtie2,
565 resulting in one count table containing the reads for beech and fungi. On average, 61 %
566 of the reads could be mapped (45 % to beech and 16 % to fungi) (Table S6). The raw
567 count table was split into a beech transcriptome count table and fungal transcriptome
568 count table. Normalization of the raw count tables and differential expression analyses
569 relative to the control was conducted using the DESeq2 package (119), implemented in
570 R (120). Differential expression analysis of the fungi was performed at the
571 metatranscriptome level (i.e., the fungal raw count tables were aggregated by their
572 EuKaryotic Orthologous Groups of protein identifiers (KOGs, https://img.jgi.doe.gov/)),
573 dropping taxon-specific information for the gene models. Two fungal
574 metatranscriptomes were considered: the full list fungi metatranscriptome (17 fungi) or
575 the ectomycorrhizal-specific metatranscriptome (13 fungi). Gene models (European
576 beech) or KOGs (fungal metatranscriptomes) with a Benjamini-Hochberg adjusted false
577 discovery rate $P_{adjusted} < 0.05$ (121) and at least 2-fold change were considered as
578 significant differentially expressed gene models (DEGs) or significant KOGs. The
579 Enzyme Commission numbers assigned to the ectomycorrhizal fungal
580 metatranscriptome were mapped to the Kyoto Encyclopedia of Genes and Genomes
581 (KEGG) metabolic pathways against *L. bicolor* in KEGG Mapper (122). Functional
582 enrichment analysis of fungal expressed genes was carried out in g:Profiler (123)
583 against KEGG metabolic pathways with *Aspergillus oryzae* as reference since the

584 model ectomycorrhizal fungus *L. bicolor* was not available. Since a main interest in our
585 experiment was to obtain information on fungal N uptake and metabolism, we manually
586 searched the complete fungal transcriptional database (Data set 2) for N-related
587 transporters and enzymes using the key words “nitrate transporter,” “nitrate reductase,”
588 “nitrite transporter,” “nitrite reductase,” “ammonium transporter”, “glutamine synthetase,”
589 “glutamate synthase” and “glutamate dehydrogenase.” These terms were searched in
590 the definition lines accompanying the annotations of each of the fungal transcripts:
591 “kogdefline” = definition of the KOG identifiers, “ECnumDef” = definition of EC number,
592 “iprDesc” = description of the InterPro identifiers, and “goName” = description of the
593 Gene Ontology term. Cluster analyses was done in Clustvis (124). Gene Ontology term
594 enrichment analysis of beech DEGs was also performed in g:Profiler (123). In addition,
595 over-representation analysis of biological pathways based on the MapMan bin
596 classification (Ath_AGI_LOCUS_TAIR10_Aug2012) of beech DEGs was performed
597 using the Classification SuperViewer Tool (125) from the Bio-Analytic Resource for
598 Plant Biology (http://bar.utoronto.ca/).

599 **Statistical analyses.** The fungal community data were Hellinger-transformed
600 and fitted into a non-metric multidimensional scaling (nMDS) ordination based on Bray-
601 Curtis dissimilarity using the ‘vegan’ package version 2.5-6 (126) and ‘ggplot2’ function
602 (127) in the R software (128). Permutational analysis of variance (‘adonis 2’) was used
603 to test if the treatments resulted in significant effects on the fungal community or
604 transcript composition. Quasi-Poisson regression models were used for over-dispersed
605 count data (e.g., species richness) and general linear models were applied to normal
606 distributed data, followed by Tukey’s HSD post-hoc test with the ‘multcomp’ package

(129). When necessary, the data was transformed to meet normal distribution. If not indicated otherwise, data are shown as means (± SD). Linear regression analysis was conducted in R (128). One cosm from ammonium and one from nitrate treatment were excluded from the ^{15}N analyses since the measured ^{15}N values in soil were higher than the amount of added ^{15}N.

Data availability statement. Raw sequences from the fungal ITS2 gene metabarcoding-Illumina sequencing are available in the Sequence Read Archive from the National Center for Biotechnology Information under BioProject accession number PRJNA736215 (130). Raw read data from RNA seq are also available at the ArrayExpress database under accession number E-MTAB-8931 (131). Additional supporting data (Data set 1-6) are accessible in Dryad (132).

SUPPLEMENTAL MATERIAL

Table S1, Table S2, Table S3, Table S4, Table S5, Table S6, Figure S1, Text S1

SUPPORTING DATA

Data_set_1_rarefied_fungal_otu_table.xlsx

Data_set_2_raw_rna_counts_fungi.xlsx

Data_set_3_normalized_rna_counts_fungal_metatranscriptomes.xlsx

Data_set_4_raw_rna_counts_fagus.xlsx

Data_set_5_normalized_rna_counts_fagus.xlsx

Data_set_6_plant_nutrients_and_environmental_conditions.xlsx

ACKNOWLEDGEMENTS

This research was funded by the German Research Foundation (DFG) through the Research Training Group 2300 “Enrichment of European Beech Forests with Conifers” (contract number: 316045089, project SP4). We thank the Göhrde State Forest management office for authorizing tree collection in the forest. CARP is grateful to Dr. Serena Müller for assistance coordinating field work, to Michael Reichel, Ronny Thoms and Jonas Glatthorn for help collecting the trees in the forest, and Gaby Lehmann for help measuring ammonium/nitrate in soil.

CARP: Conceptualization, Methodology, Project administration, Investigation, Formal analysis, Writing – original draft, Writing – review & editing. DJ, DS, RD: Data curation, Writing – review & editing. AP: Conceptualization, Methodology, Formal analysis, Supervision, Writing – review & editing.

We declare no competing interests.

REFERENCES

1. LeBauer DS, Treseder KK. 2008. Nitrogen limitation of net primary productivity in terrestrial ecosystems is globally distributed. Ecology 89:371–379.
2. Du E, Terrer C, Pellegrini AFA, Ahlström A, van Lissa CJ, Zhao X, Xia N, Wu X, Jackson RB. 2020. Global patterns of terrestrial nitrogen and phosphorus limitation. Nat Geosci 13:221–226.
3. JOSHUA P. SCHIMEL AJB. 2004. NITROGEN MINERALIZATION: CHALLENGES OF A CHANGING PARADIGM. Ecology 85:591–602.
4. Rennenberg H, Dannenmann M, Gessler A, Kreuzwieser J, Simon J, Papen H. 2009. Nitrogen balance in forest soils: Nutritional limitation of plants under climate change stresses. Plant Biol 11:4–23.

651 5. Nieder R, Benbi DK, Scherer HW. 2011. Fixation and defixation of ammonium in
652 soils: A review. Biol Fertil Soils 47:1–14.
653 6. Rennenberg H, Dannenmann M. 2015. Nitrogen Nutrition of Trees in Temperate
654 Forests—The Significance of Nitrogen Availability in the Pedosphere and
655 Atmosphere. Forests 6:2820–2835.
656 7. Roth M, Michiels HG, Puhlmann H, Sucker C, Winter MB, Hauck M. 2020.
657 Responses of Temperate Forests to Nitrogen Deposition: Testing the Explanatory
658 Power of Modeled Deposition Datasets for Vegetation Gradients. Ecosystems
659 https://doi.org/10.1007/s10021-020-00579-4.
660 8. Vitousek P et al. 1997. HUMAN ALTERATION OF THE GLOBAL NITROGEN
661 CYCLE: SOURCES AND CONSEQUENCES. Ecol Appl 3:737–750.
662 9. Erisman JW, van Grinsven H, Grizzetti B, Bouraoui F, Powlson D, Sutton MA,
663 Bleeker A, Reis S. 2011. The European nitrogen problem in a global perspective.
664 Eur Nitrogen Assess 9–31.
665 10. Fowler D, Coyle M, Skiba U, Sutton MA, Cape JN, Reis S, Sheppard LJ, Jenkins
666 A, Grizzetti B, Galloway JN, Vitousek P, Leach A, Bouwman AF, Butterbach-Bahl
667 K, Dentener F, Stevenson D, Amann M, Voss M. 2013. The global nitrogen cycle
668 in the Twentyfirst century. Philos Trans R Soc B Biol Sci 368.
669 11. Galloway JN, Leach AM, Bleeker A, Erisman JW. 2013. A chronology of human
670 understanding of the nitrogen cycle. Philos Trans R Soc B Biol Sci 368.
671 12. Fleck S, Eickenscheidt N, Ahrends B, Evers J, Grüneberg E, Ziche D, Höhle J,
672 Schmitz A, Weis W, Schmidt-Walter P, Andreae H, Wellbrock N. 2019. Nitrogen
673 Status and Dynamics in German Forest Soils, p. 123–166. *In* . Cham.

13. Kadyampakeni DM, Nkedi-Kizza P, Leiva JA, Muwamba A, Fletcher E, Morgan KT. 2018. Ammonium and nitrate transport during saturated and unsaturated water flow through sandy soils. J Plant Nutr Soil Sci 181:198–210.

14. Brady NC, Weil RR. 1999. Nitrogen and Sulfure Economy of Soils, p. 491–539. *In* The Nature and Properties of Soils12th ed. Prentice-Hall, Inc., New Jersey.

15. Read DJ, Perez-Moreno J. 2003. Mycorrhizas and nutrient cycling in ecosystems - A journey towards relevance? New Phytol 157:475–492.

16. Hobbie JE, Hobbie EA. 2006. 15N in symbiotic fungi and plants estimates nitrogen and carbon flux rates in arctic tundra. Ecology 87:816–822.

17. Hobbie EA, Hobbie JE. 2008. Natural Abundance of 15N in Nitrogen-Limited Forests and Tundra Can Estimate Nitrogen Cycling Through Mycorrhizal Fungi: A Review. Ecosystems 11:815–830.

18. Rineau F, Roth D, Shah F, Smits M, Johansson T, Canbäck B, Olsen PB, Persson P, Grell MN, Lindquist E, Grigoriev I V., Lange L, Tunlid A. 2012. The ectomycorrhizal fungus Paxillus involutus converts organic matter in plant litter using a trimmed brown-rot mechanism involving Fenton chemistry. Environ Microbiol 14:1477–1487.

19. van der Heijden MGA, Martin FM, Selosse M-A, Sanders IR. 2015. Mycorrhizal ecology and evolution: the past, the present, and the future. New Phytol 205:1406–1423.

20. Op De Beeck M, Troein C, Peterson C, Persson P, Tunlid A. 2018. Fenton reaction facilitates organic nitrogen acquisition by an ectomycorrhizal fungus. New Phytol 218:335–343.

21. Buée M, Vairelles D, Garbaye J. 2005. Year-round monitoring of diversity and potential metabolic activity of the ectomycorrhizal community in a beech (Fagus silvatica) forest subjected to two thinning regimes. Mycorrhiza 15:235–245.

22. Pena R, Offermann C, Simon J, Naumann PS, Ge??ler A, Holst J, Dannenmann M, Mayer H, K??gel-Knabner I, Rennenberg H, Polle A. 2010. Girdling affects ectomycorrhizal fungal (EMF) diversity and reveals functional differences in EMF community composition in a beech forest. Appl Environ Microbiol 76:1831–1841.

23. Lang C, Polle A. 2011. Ectomycorrhizal fungal diversity, tree diversity and root nutrient relations in a mixed Central European forest. Tree Physiol 31:531–538.

24. Schröter K, Wemheuer B, Pena R, Schöning I, Ehbrecht M, Schall P, Ammer C, Daniel R, Polle A. 2019. Assembly processes of trophic guilds in the root mycobiome of temperate forests. Mol Ecol 28:348–364.

25. Melin E, Nilsson H. 1957. Transport of C14-labelled Photosynthate to the Fungal Associate of Pine Mycorrhiza. Sven Bot Tidskr 51:166–186.

26. Melin E, Nilsson H. 1952. Transport of labelled nitrogen from an ammonium source to pine seedlings through mycorrhizal mycelium. Sven Bot Tidskr 46:281–285.

27. Pena R, Polle A. 2014. Attributing functions to ectomycorrhizal fungal identities in assemblages for nitrogen acquisition under stress. ISME J 8:321–330.

28. Pena R, Tejedor J, Zeller B, Dannenmann M, Polle A. 2013. Interspecific temporal and spatial differences in the acquisition of litter-derived nitrogen by ectomycorrhizal fungal assemblages. New Phytol 199:520–528.

29. FINLAY RD, EK H, ODHAM G, SÖDERSTRÖM B. 1988. Mycelial uptake,

translocation and assimilation of nitrogen from 15N-labelled ammonium by Pinus sylvestris plants infected with four different ectomycorrhizal fungi. New Phytol 110:59–66.

30. FINLAY RD, EK H, ODHAM G, SÜDERSTRÖM B. 1989. Uptake, translocation and assimilation of nitrogen from 15N-labelled ammonium and nitrate sources by intact ectomycorrhizal systems of Fagus sylvatica infected with Paxillus involutus. New Phytol 113:47–55.

31. EK H, ANDERSSON S, ARNEBRANT K, SÖDERSTRÖM B. 1994. Growth and assimilation of NH4+ and NO3− by Paxillus involutus in association with Betula pendula and Picea abies as affected by substrate pH. New Phytol 128:629–637.

32. Dannenmann M, Bimüller C, Gschwendtner S, Leberecht M, Tejedor J, Bilela S, Gasche R, Hanewinkel M, Baltensweiler A, Kögel-Knabner I, Polle A, Schloter M, Simon J, Rennenberg H. 2016. Climate change impairs nitrogen cycling in european beech forests. PLoS One 11:1–24.

33. Leberecht M, Dannenmann M, Tejedor J, Simon J, Rennenberg H, Polle A. 2016. Segregation of nitrogen use between ammonium and nitrate of ectomycorrhizas and beech trees. Plant Cell Environ 39:2691–2700.

34. FINLAY RD, FROSTEGÅRD, SONNERFELDT A -M. 1992. Utilization of organic and inorganic nitrogen sources by ectomycorrhizal fungi in pure culture and in symbiosis with Pinus contorta Dougl. ex Loud. New Phytol 120:105–115.

35. Nygren CMR, Eberhardt U, Karlsson M, Parrent JL, Lindahl BD, Taylor AFS. 2008. Growth on nitrate and occurrence of nitrate reductase-encoding genes in a phylogenetically diverse range of ectomycorrhizal fungi. New Phytol 180:875–889.

743 36. Kemppainen M, Duplessis S, Martin F, Pardo AG. 2009. RNA silencing in the
744 model mycorrhizal fungus Laccaria bicolor : gene knock-down of nitrate reductase
745 results in inhibition of symbiosis with Populus. Environ Microbiol 11:1878–1896.
746 37. Chalot M, Blaudez D, Brun A. 2006. Ammonia: a candidate for nitrogen transfer at
747 the mycorrhizal interface. Trends Plant Sci.
748 38. Casieri L, Ait Lahmidi N, Doidy J, Veneault-Fourrey C, Migeon A, Bonneau L,
749 Courty PE, Garcia K, Charbonnier M, Delteil A, Brun A, Zimmermann S, Plassard
750 C, Wipf D. 2013. Biotrophic transportome in mutualistic plant-fungal interactions.
751 Mycorrhiza 23:597–625.
752 39. Garcia K, Doidy J, Zimmermann SD, Wipf D, Courty PE. 2016. Take a Trip
753 Through the Plant and Fungal Transportome of Mycorrhiza. Trends Plant Sci
754 21:937–950.
755 40. Nehls U, Plassard C. 2018. Nitrogen and phosphate metabolism in
756 ectomycorrhizas. New Phytol 1047–1058.
757 41. Becquer A, Guerrero-Galán C, Eibensteiner JL, Houdinet G, Bücking H,
758 Zimmermann SD, Garcia K. 2019. The ectomycorrhizal contribution to tree
759 nutrition. Adv Bot Res 89:77–126.
760 42. Stuart EK, Plett KL. 2020. Digging Deeper: In Search of the Mechanisms of
761 Carbon and Nitrogen Exchange in Ectomycorrhizal Symbioses. Front Plant Sci.
762 Frontiers Media S.A.
763 43. Selle A, Willmann M, Grunze N, Geßler A, Weiß M, Nehls U. 2005. The high-
764 affinity poplar ammonium importer PttAMT1.2 and its role in ectomycorrhizal
765 symbiosis. New Phytol 168:697–706.

766 44. Lucic E, Fourrey C, Kohler A, Martin F, Chalot M, Brun-Jacob A. 2008. A gene
767 repertoire for nitrogen transporters in Laccaria bicolor. New Phytol 180:343–364.
768 45. Dietz S, von Bülow J, Beitz E, Nehls U. 2011. The aquaporin gene family of the
769 ectomycorrhizal fungus Laccaria bicolor: Lessons for symbiotic functions. New
770 Phytol 190:927–940.
771 46. Hacquard S, Tisserant E, Brun A, Legué V, Martin F, Kohler A. 2013. Laser
772 microdissection and microarray analysis of Tuber melanosporum ectomycorrhizas
773 reveal functional heterogeneity between mantle and Hartig net compartments.
774 Environ Microbiol 15:1853–1869.
775 47. Müller T, Avolio M, Olivi M, Benjdia M, Rikirsch E, Kasaras A, Fitz M, Chalot M,
776 Wipf D. 2007. Nitrogen transport in the ectomycorrhiza association: The
777 Hebeloma cylindrosporum-Pinus pinaster model. Phytochemistry 68:41–51.
778 48. Willmann A, Thomfohrde S, Haensch R, Nehls U. 2014. The poplar NRT2 gene
779 family of high affinity nitrate importers: Impact of nitrogen nutrition and
780 ectomycorrhiza formation. Environ Exp Bot 108:79–88.
781 49. Sa G, Yao J, Deng C, Liu J, Zhang Y, Zhu Z, Zhang Y, Ma X, Zhao R, Lin S, Lu
782 C, Polle A, Chen S. 2019. Amelioration of nitrate uptake under salt stress by
783 ectomycorrhiza with and without a Hartig net. New Phytol 222:1951–1964.
784 50. Javelle A, Morel M, Rodríguez-Pastrana BR, Botton B, André B, Marini AM, Brun
785 A, Chalot M. 2003. Molecular characterization, function and regulation of
786 ammonium transporters (Amt) and ammonium-metabolizing enzymes (GS,
787 NADP-GDH) in the ectomycorrhizal fungus Hebeloma cylindrosporum. Mol
788 Microbiol 47:411–430.

789 51. A. Lal M. 2018. Nitrogen Metabolism, p. 425–480. *In* Plant Physiology,
790 Development and Metabolism. Springer Singapore, Singapore.
791 52. MARTIN F, CÕTÉ R, CANET D. 1994. NH4+ assimilation in the ectomycorrhizal
792 basidiomycete Laccaria bicolor (Maire) Orton, a 15N-NMR study. New Phytol
793 128:479–485.
794 53. Vallorani L, Polidori E, Sacconi C, Agostini D, Pierleoni R, Piccoli G, Zeppa S,
795 Stocchi V. 2002. Biochemical and molecular characterization of NADP-glutamate
796 dehydrogenase from the ectomycorrhizal fungus Tuber borchii. New Phytol
797 154:779–790.
798 54. Morel M, Buée M, Chalot M, Brun A. 2006. NADP-dependent glutamate
799 dehydrogenase: A dispensable function in ectomycorrhizal fungi. New Phytol
800 169:179–190.
801 55. Grzechowiak M, Sliwiak J, Jaskolski M, Ruszkowski M. 2020. Structural Studies
802 of Glutamate Dehydrogenase (Isoform 1) From Arabidopsis thaliana, an Important
803 Enzyme at the Branch-Point Between Carbon and Nitrogen Metabolism. Front
804 Plant Sci 11:1–17.
805 56. Grigoriev I V., Nikitin R, Haridas S, Kuo A, Ohm R, Otillar R, Riley R, Salamov A,
806 Zhao X, Korzeniewski F, Smirnova T, Nordberg H, Dubchak I, Shabalov I. 2014.
807 MycoCosm portal: Gearing up for 1000 fungal genomes. Nucleic Acids Res
808 42:699–704.
809 57. Mishra B, Gupta DK, Pfenninger M, Hickler T, Langer E, Nam B, Paule J, Sharma
810 R, Ulaszewski B, Warmbier J, Burczyk J, Thines M. 2018. A reference genome of
811 the European beech (Fagus sylvatica L.). Gigascience 7.

812 58. Meesenburg H, Ahrends B, Fleck S, Wagner M, Fortmann H, Scheler B, Klinck U,
813 Dammann I, Eichhorn J, Mindrup M, Meiwes KJ. 2016. Long-term changes of
814 ecosystem services at Solling, Germany: Recovery from acidification, but
815 increasing nitrogen saturation? Ecol Indic 65:103–112.
816 59. de Vries W, Du E, Butterbach-Bahl K. 2014. Short and long-term impacts of
817 nitrogen deposition on carbon sequestration by forest ecosystems. Curr Opin
818 Environ Sustain 9–10:90–104.
819 60. Green ML, Karp PD. 2005. Genome annotation errors in pathway databases due
820 to semantic ambiguity in partial EC numbers. Nucleic Acids Res 33:4035–4039.
821 61. Schilmiller AL, Stout J, Weng JK, Humphreys J, Ruegger MO, Chapple C. 2009.
822 Mutations in the cinnamate 4-hydroxylase gene impact metabolism, growth and
823 development in Arabidopsis. Plant J 60:771–782.
824 62. Chandler J, Wilson A, Dean C. 1996. Arabidopsis mutants showing an altered
825 response to vernalization. Plant J 10:637–644.
826 63. Peng FY, Weselake RJ. 2013. Genome-wide identification and analysis of the B3
827 superfamily of transcription factors in Brassicaceae and major crop plants. Theor
828 Appl Genet 126:1305–1319.
829 64. Bianchet C, Wong A, Quaglia M, Alqurashi M, Gehring C, Ntoukakis V, Pasqualini
830 S. 2019. An Arabidopsis thaliana leucine-rich repeat protein harbors an adenylyl
831 cyclase catalytic center and affects responses to pathogens. J Plant Physiol
832 232:12–22.
833 65. Lin SH, Kuo HF, Canivenc G, Lin CS, Lepetit M, Hsu PK, Tillard P, Lin HG, Wang
834 YY, Tsai CB, Gojon A, Tsay YF. 2008. Mutation of the Arabidopsis NRT1.5 nitrate

transporter causes defective root-to-shoot nitrate transport. Plant Cell 20:2514–2528.

66. Maeda SI, Konishi M, Yanagisawa S, Omata T. 2014. Nitrite transport activity of a novel HPP family protein conserved in cyanobacteria and chloroplasts. Plant Cell Physiol 55:1311–1324.

67. Hachiya T, Ueda N, Kitagawa M, Hanke G, Suzuki A, Hase T, Sakakibara H. 2016. Arabidopsis root-type ferredoxin: NADP(H) oxidoreductase 2 is involved in detoxification of nitrite in roots. Plant Cell Physiol 57:2440–2450.

68. Gross J, Won KC, Lezhneva L, Falk J, Krupinska K, Shinozaki K, Seki M, Herrmann RG, Meurer J. 2006. A plant locus essential for phylloquinone (vitamin K1) biosynthesis originated from a fusion of four eubacterial genes. J Biol Chem 281:17189–17196.

69. Wildermuth MC, Dewdney J, Wu G, Ausubel FM. 2002. Erratum: corrigendum: Isochorismate synthase is required to synthesize salicylic acid for plant defence. Nature 417:571–571.

70. Garcion C, Lohmann A, Lamodière E, Catinot J, Buchala A, Doermann P, Métraux JP. 2008. Characterization and biological function of the Isochorismate Synthase2 gene of Arabidopsis. Plant Physiol 147:1279–1287.

71. Hartmann M, Zeier J. 2018. l-lysine metabolism to N-hydroxypipecolic acid: an integral immune-activating pathway in plants. Plant J 96:5–21.

72. Dannenmann M, Simon J, Gasche R, Holst J, Naumann PS, Kögel-Knabner I, Knicker H, Mayer H, Schloter M, Pena R, Polle A, Rennenberg H, Papen H. 2009. Tree girdling provides insight on the role of labile carbon in nitrogen partitioning

858 between soil microorganisms and adult European beech. Soil Biol Biochem
859 41:1622–1631.
860 73. Unuk T, Martinović T, Finžgar D, Šibanc N, Grebenc T, Kraigher H. 2019. Root-
861 associated fungal communities from two phenologically contrasting silver fir
862 (Abies alba mill.) groups of trees. Front Plant Sci 10:1–11.
863 74. Mrak T, Hukić E, Štraus I, Unuk Nahberger T, Kraigher H. 2020. Ectomycorrhizal
864 community composition of organic and mineral soil horizons in silver fir (Abies
865 alba Mill.) stands. Mycorrhiza 30:541–553.
866 75. Lilleskov EA, Bruns TD. 2003. Root colonization dynamics of two ectomycorrhizal
867 fungi of contrasting life history strategies are mediated by addition of organic
868 nutrient patches. New Phytol 159:141–151.
869 76. Malajczuk N, Lapeyrie F, Garbaye J. 1990. Infectivity of pine and eucalypt isolates
870 of Pisolithus tinctorius (Pers.) Coker & Couch on roots of Eucalyptus
871 urophylla S. T. Blake in vitro. II. Ultrastructural and biochemical changes at the
872 early stage of mycorrhiza formation. New Phytol 116:115–122.
873 77. Treseder KK. 2004. A meta-analysis of mycorrhizal responses to nitrogen,
874 phosphorus, and atmospheric CO2 in field studies. New Phytol 164:347–355.
875 78. Lilleskov EA, Hobbie EA, Horton TR. 2011. Conservation of ectomycorrhizal fungi:
876 Exploring the linkages between functional and taxonomic responses to
877 anthropogenic N deposition. Fungal Ecol 4:174–183.
878 79. Cox F, Barsoum N, Lilleskov EA, Bidartondo MI. 2010. Nitrogen availability is a
879 primary determinant of conifer mycorrhizas across complex environmental
880 gradients. Ecol Lett 13:1103–1113.

881 80. de Witte LC, Rosenstock NP, van der Linde S, Braun S. 2017. Nitrogen
882 deposition changes ectomycorrhizal communities in Swiss beech forests. Sci
883 Total Environ 605–606:1083–1096.
884 81. van der Linde S, Suz LM, Orme CDL, Cox F, Andreae H, Asi E, Atkinson B,
885 Benham S, Carroll C, Cools N, De Vos B, Dietrich H-P, Eichhorn J, Gehrmann J,
886 Grebenc T, Gweon HS, Hansen K, Jacob F, Kristofel F, Lech P, Manninger M,
887 Martin J, Meesenburg H, Merila P, Nicolas M, Pavlenda P, Rautio P, Schaub M,
888 Schrock H-W, Seidling W, Šramek V, Thimonier A, Thomsen IM, Titeux H,
889 Vanguelova E, Verstraeten A, Vesterdal L, Waldner P, Wijk S, Zhang Y, Žlindra
890 D, Bidartondo MI. 2018. Author Correction: Environment and host as large-scale
891 controls of ectomycorrhizal fungi. Nature 561:E42–E42.
892 82. Peter M, Kohler A, Ohm RA, Kuo A, Krützmann J, Morin E, Arend M, Barry KW,
893 Binder M, Choi C, Clum A, Copeland A, Grisel N, Haridas S, Kipfer T, Labutti K,
894 Lindquist E, Lipzen A, Maire R, Meier B, Mihaltcheva S, Molinier V, Murat C,
895 Pöggeler S, Quandt CA, Sperisen C, Tritt A, Tisserant E, Crous PW, Henrissat B,
896 Nehls U, Egli S, Spatafora JW, Grigoriev I V., Martin FM. 2016. Ectomycorrhizal
897 ecology is imprinted in the genome of the dominant symbiotic fungus
898 Cenococcum geophilum. Nat Commun 7.
899 83. Trocha LK, Bułaj B, Durska A, Frankowski M, Mucha J. 2021. Not all long-
900 distance-exploration types of ectomycorrhizae are the same: Differential
901 accumulation of nitrogen and carbon in scleroderma and Xerocomus in response
902 to variations in soil fertility. IForest 14:48–52.
903 84. Kothawala DN, Moore TR. 2009. Adsorption of dissolved nitrogen by forest

mineral soils. Can J For Res 39:2381–2390.

85. Clark DR, McKew BA, Dong LF, Leung G, Dumbrell AJ, Stott A, Grant H, Nedwell DB, Trimmer M, Whitby C. 2020. Mineralization and nitrification: Archaea dominate ammonia-oxidising communities in grassland soils. Soil Biol Biochem 143:107725.

86. Li X, Rennenberg H, Simon J. 2016. Seasonal variation in N uptake strategies in the understorey of a beech-dominated N-limited forest ecosystem depends on N source and species. Tree Physiol 36:589–600.

87. Jargeat P, Gay G, Debaud JC, Marmeisse R. 2000. Transcription of a nitrate reductase gene isolated from the symbiotic basidiomycete fungus Hebeloma cylindrosporum does not require induction by nitrate. Mol Gen Genet 263:948–956.

88. Jargeat P, Rekangalt D, Verner MC, Gay G, Debaud JC, Marmeisse R, Fraissinet-Tachet L. 2003. Characterisation and expression analysis of a nitrate transporter and nitrite reductase genes, two members of a gene cluster for nitrate assimilation from the symbiotic basidiomycete Hebeloma cylindrosporum. Curr Genet 43:199–205.

89. Montanini B, Viscomi AR, Bolchi A, Martin Y, Siverio JM, Balestrini R, Bonfante P, Ottonello S. 2006. Functional properties and differential mode of regulation of the nitrate transporter from a plant symbiotic ascomycete. Biochem J 394:125–134.

90. Guescini M, Zeppa S, Pierleoni R, Sisti D, Stocchi L, Stocchi V. 2007. The expression profile of the Tuber borchii nitrite reductase suggests its positive contribution to host plant nitrogen nutrition. Curr Genet 51:31–41.

927 91. Kemppainen MJ, Alvarez Crespo MC, Pardo AG. 2010. fHANT-AC genes of the
928 ectomycorrhizal fungus Laccaria bicolor are not repressed by L-glutamine
929 allowing simultaneous utilization of nitrate and organic nitrogen sources. Environ
930 Microbiol Rep 2:541–553.
931 92. Javelle A, Rodríguez-Pastrana BR, Jacob C, Botton B, Brun A, André B, Marini
932 AM, Chalot M. 2001. Molecular characterization of two ammonium transporters
933 from the ectomycorrhizal fungus Hebeloma cylindrosporum. FEBS Lett 505:393–
934 398.
935 93. Willmann A, Weiß M, Nehls U. 2007. Ectomycorrhiza-mediated repression of the
936 high-affinity ammonium importer gene AmAMT2 in Amanita muscaria. Curr Genet
937 51:71–78.
938 94. Kranabetter JM, Hawkins BJ, Jones MD, Robbins S, Dyer T, Li T. 2015. Species
939 turnover (??-diversity) in ectomycorrhizal fungi linked to NH 4 + uptake capacity.
940 Mol Ecol 24:5992–6005.
941 95. Patterson K, Cakmak T, Cooper A, Lager I, Rasmusson AG, Escobar MA. 2010.
942 Distinct signalling pathways and transcriptome response signatures differentiate
943 ammonium- and nitrate-supplied plants. Plant, Cell Environ 33:1486–1501.
944 96. Lima JE, Kojima S, Takahashi H, von Wirén N. 2010. Ammonium triggers lateral
945 root branching in Arabidopsis in an AMMONIUM TRANSPORTER1;3-dependent
946 manner. Plant Cell 22:3621–3633.
947 97. Xu N, Wang R, Zhao L, Zhang C, Li Z, Lei Z, Liu F, Guan P, Chu Z, Crawford NM.
948 2015. The arabidopsis NRG2 protein mediates nitrate signaling and interacts with
949 and regulates key nitrate regulators. Plant Cell 28:485–504.

950 98. O'Brien JAA, Vega A, Bouguyon E, Krouk G, Gojon A, Coruzzi G, Gutiérrez RAA.
951 2016. Nitrate Transport, Sensing, and Responses in Plants. Mol Plant 9:837–856.
952 99. Hachiya T, Sakakibara H. 2017. Interactions between nitrate and ammonium in
953 their uptake, allocation, assimilation, and signaling in plants. J Exp Bot 68:2501–
954 2512.
955 100. Asim M, Ullah Z, Xu F, An L, Aluko OO, Wang Q, Liu H. 2020. Nitrate Signaling,
956 Functions, and Regulation of Root System Architecture: Insights from Arabidopsis
957 thaliana. Genes (Basel) 11:633.
958 101. Schwarz G, Mendel RR. 2006. Molybdenum cofactor biosynthesis and
959 molybdenum enzymes. Annu Rev Plant Biol 57:623–647.
960 102. Kasper K, Abreu IN, Freussner K, Zienkiewsicz K, Herrfurth C, Ischebeck T, Janz
961 D, Majcherczyk An, Schmitt K, Valerius O, Braus GH, Feussner I, Polle A. 2021.
962 Multi-omics analysis of xylem sap uncovers dynamic modulation of poplar
963 defenses by ammonium and nitratebioRxiv.
964 103. Chen K, Fan B, Du L, Chen Z. 2004. Activation of hypersensitive cell death by
965 pathogen-induced receptor-like protein kinases from Arabidopsis. Plant Mol Biol
966 56:271–283.
967 104. Quezada EH, García GX, Arthikala MK, Melappa G, Lara M, Nanjareddy K. 2019.
968 Cysteine-rich receptor-like kinase gene family identification in the phaseolus
969 genome and comparative analysis of their expression profiles specific to
970 mycorrhizal and rhizobial symbiosis. Genes (Basel) 10.
971 105. Klepikova A V., Kasianov AS, Gerasimov ES, Logacheva MD, Penin AA. 2016. A
972 high resolution map of the Arabidopsis thaliana developmental transcriptome

973 based on RNA-seq profiling. Plant J 88:1058–1070.
974 106. Boess J, Gehrt E, Müller U, Ostmann U, Sbresny J, Steininger A. 2004.
975 Erläuterungsheft zur digitalen nutzungsdifferenzierten Bodenkundlichen
976 Übersichtskarte 1:50.000 (BÜK50n) von Niedersachsen. Schweizerbart Science
977 Publishers, Stuttgart, Germany.
978 107. Roloff A. 1988. Morphologie der Kronenentwicklung von Fagus sylvatica L.
979 (Rotbuche) unter besonderer Berücksichtigung neuartiger Veränderungen: II.
980 Strategie der Luftraumeroberung und Veränderungen durch Umwelteinflüsse.
981 Flora 180:297–338.
982 108. König N. 2014. Handbuch Forstliche Analytik: Eine Loseblatt-Sammlung der
983 Analysemethoden im Forstbereich.
984 109. Hachiya T, Okamoto Y. 2017. Simple Spectroscopic Determination of Nitrate,
985 Nitrite, and Ammonium in Arabidopsis thaliana. BIO-PROTOCOL 7.
986 110. Schopfer P. 1989. Qualitative und quantitative Analyse von Pflanzenmaterial, p.
987 1–51. *In* Experimentelle Pflanzenphysiologie. Springer Berlin Heidelberg, Berlin,
988 Heidelberg.
989 111. Toju H, Tanabe AS, Yamamoto S, Sato H. 2012. High-coverage ITS primers for
990 the DNA-based identification of ascomycetes and basidiomycetes in
991 environmental samples. PLoS One 7.
992 112. White TJ, Bruns T, Lee S, Taylor J. 1990. AMPLIFICATION AND DIRECT
993 SEQUENCING OF FUNGAL RIBOSOMAL RNA GENES FOR
994 PHYLOGENETICS, p. 315–322. *In* Innis, MA, Gelfand, DH, Sninsky, JJ, White,
995 TJ (eds.), PCR Protocols. Elsevier, San Diego.

113. Abarenkov K, Zirk A, Piirmann T, Pöhönen R, Ivanov F, Nilsson RH, Kõljalg U. 2020. Full UNITE+INSD dataset for Fungi. UNITE Community.

114. Altschul SF, Gish W, Miller W, Myers EW, Lipman DJ. 1990. Basic local alignment search tool. J Mol Biol 215:403–410.

115. Nguyen NH, Song Z, Bates ST, Branco S, Tedersoo L, Menke J, Schilling JS, Kennedy PG. 2016. FUNGuild: An open annotation tool for parsing fungal community datasets by ecological guild. Fungal Ecol 20:241–248.

116. Andersen K, Kirkegaard R, Karst S, Albertsen M. 2018. ampvis2: an R package to analyse and visualise 16S rRNA amplicon data. bioRxiv 299537.

117. Chang S, Puryear J, Cairney J. 1993. A simple and efficient method for isolating RNA from pine trees. Plant Mol Biol Report 11:113–116.

118. Langmead B, Salzberg SL. 2012. Fast gapped-read alignment with Bowtie 2. Nat Methods 9:357–359.

119. Love MI, Huber W, Anders S. 2014. Moderated estimation of fold change and dispersion for RNA-seq data with DESeq2. Genome Biol 15:1–21.

120. R Core Team. 2018. R: A language and environment for statistical computing. R Foundation for Statistical Computing, Vienna, Austria.

121. Benjamini Y, Hochberg Y. 1995. Controlling the False Discovery Rate : A Practical and Powerful Approach to Multiple Testing. R Stat Soc 57:289–300.

122. Kanehisa M, Sato Y. 2020. KEGG Mapper for inferring cellular functions from protein sequences. Protein Sci 29:28–35.

123. Raudvere U, Kolberg L, Kuzmin I, Arak T, Adler P, Peterson H, Vilo J. 2019. G:Profiler: A web server for functional enrichment analysis and conversions of

gene lists (2019 update). Nucleic Acids Res 47:W191–W198.

124. Metsalu T, Vilo J. 2015. ClustVis: A web tool for visualizing clustering of multivariate data using Principal Component Analysis and heatmap. Nucleic Acids Res 43:W566–W570.

125. Provart N, Zhu T. 2003. A Browser-based Functional Classification SuperViewer for Arabidopsis Genomics. Curr Comput Mol Biol 271–272.

126. Oksanen J, Blanchet FG, Friendly M, Kindt R, Legendre P, McGlinn D, Minchin PR, O'Hara RB, Simpson GL, Solymos P, Stevens MHH, Szoecs E, Wagner H. 2019. vegan: Community Ecology Package.

127. Wickham H. 2016. ggplot2: Elegant Graphics for Data Analysis. Springer-Verlag, New York.

128. R Core Team. 2020. R: A Language and Environment for Statistical Computing. R Foundation for Statistical Computing, Vienna, Austria.

129. Hothorn T, Bretz F, Westfall P. 2008. Simultaneous Inference in General Parametric Models. Biometrical J 50:346–363.

130. Rivera Pérez CA, Schneider D, Daniel R, Polle A. 2021. Characterization of root fungal community of European beech saplings. Seq Read Arch (SRA) https//www.ncbi.nlm.nih.gov/bioproject/736215.

131. Rivera Pérez CA, Janz D, Polle A. 2020. Transcription profiling of mycorrhized European beech (Fagus sylvatica L.) roots in response to fertilization with different forms of inorganic nitrogen. ArrayExpress database https://www.ebi.ac.uk/arrayexpress/experiments/E-MTAB-8931/.

132. Rivera Pérez CA, Janz D, Schneider D, Daniel R, Polle A. 2021. Mineral nitrogen

nutrition of Fagus sylvatica L roots colonized by ectomycorrhizal fungi in native forest soil. Dryad Dataset https://doi.org/105061/dryad.zpc866t8v.

133. Walker AK, Frasz SL, Seifert KA, Miller JD, Mondo SJ, LaButti K, Lipzen A, Dockter RB, Kennedy MC, Grigoriev I V., Spatafora JW. 2016. Erratum: Full genome of phialocephala scopiformis daomc 229536, a fungal endophyte of spruce producing the potent anti-insectan compound rugulosin [Genome Announcements 4, 1, (2016) (e01768-15)] DOI: 10.1128/genomeA.01768-15. Genome Announc 4:2–4.

134. Kohler A, Kuo A, Nagy LG, Morin E, Barry KW, Buscot F, Canbäck B, Choi C, Cichocki N, Clum A, Colpaert J, Copeland A, Costa MD, Doré J, Floudas D, Gay G, Girlanda M, Henrissat B, Herrmann S, Hess J, Högberg N, Johansson T, Khouja H-R, LaButti K, Lahrmann U, Levasseur A, Lindquist EA, Lipzen A, Marmeisse R, Martino E, Murat C, Ngan CY, Nehls U, Plett JM, Pringle A, Ohm RA, Perotto S, Peter M, Riley R, Rineau F, Ruytinx J, Salamov A, Shah F, Sun H, Tarkka M, Tritt A, Veneault-Fourrey C, Zuccaro A, Tunlid A, Grigoriev I V., Hibbett DS, Martin F. 2015. Convergent losses of decay mechanisms and rapid turnover of symbiosis genes in mycorrhizal mutualists. Nat Genet 47:410–415.

135. Martino E, Morin E, Grelet GA, Kuo A, Kohler A, Daghino S, Barry KW, Cichocki N, Clum A, Dockter RB, Hainaut M, Kuo RC, LaButti K, Lindahl BD, Lindquist EA, Lipzen A, Khouja HR, Magnuson J, Murat C, Ohm RA, Singer SW, Spatafora JW, Wang M, Veneault-Fourrey C, Henrissat B, Grigoriev I V., Martin FM, Perotto S. 2018. Comparative genomics and transcriptomics depict ericoid mycorrhizal fungi as versatile saprotrophs and plant mutualists. New Phytol 217:1213–1229.

136. Riley R, Salamov AA, Brown DW, Nagy LG, Floudas D, Held BW, Levasseur A, Lombard V, Morin E, Otillar R, Lindquist EA, Sun H, LaButti KM, Schmutz J, Jabbour D, Luo H, Baker SE, Pisabarro AG, Walton JD, Blanchette RA, Henrissat B, Martin F, Cullen D, Hibbett DS, Grigoriev I V. 2014. Erratum: Extensive sampling of basidiomycete genomes demonstrates inadequacy of the white-rot/brown-rot paradigm for wood decay fungi (Proceedings of the National Academy of Sciences of the United States of America (2014) 111, 27 (9923-9928) DOI: 10.1073/. Proc Natl Acad Sci U S A 111:14959.

137. Miyauchi S, Kiss E, Kuo A, Drula E, Kohler A, Sánchez-García M, Morin E, Andreopoulos B, Barry KW, Bonito G, Buée M, Carver A, Chen C, Cichocki N, Clum A, Culley D, Crous PW, Fauchery L, Girlanda M, Hayes RD, Kéri Z, LaButti K, Lipzen A, Lombard V, Magnuson J, Maillard F, Murat C, Nolan M, Ohm RA, Pangilinan J, Pereira M de F, Perotto S, Peter M, Pfister S, Riley R, Sitrit Y, Stielow JB, Szöllősi G, Žifčáková L, Štursová M, Spatafora JW, Tedersoo L, Vaario LM, Yamada A, Yan M, Wang P, Xu J, Bruns T, Baldrian P, Vilgalys R, Dunand C, Henrissat B, Grigoriev I V., Hibbett D, Nagy LG, Martin FM. 2020. Large-scale genome sequencing of mycorrhizal fungi provides insights into the early evolution of symbiotic traits. Nat Commun 11:1–17.

138. Martin F, Aerts A, Ahrén D, Brun A, Danchin EGJ, Duchaussoy F, Gibon J, Kohler A, Lindquist E, Pereda V, Salamov A, Shapiro HJ, Wuyts J, Blaudez D, Buée M, Brokstein P, Canbäck B, Cohen D, Courty PE, Coutinho PM, Delaruelle C, Detter JC, Deveau A, DiFazio S, Duplessis S, Fraissinet-Tachet L, Lucic E, Frey-Klett P, Fourrey C, Feussner I, Gay G, Grimwood J, Hoegger PJ, Jain P, Kilaru S, Labbé

J, Lin YC, Legué V, Le Tacon F, Marmeisse R, Melayah D, Montanini B, Muratet M, Nehls U, Niculita-Hirzel H, Secq MPO Le, Peter M, Quesneville H, Rajashekar B, Reich M, Rouhier N, Schmutz J, Yin T, Chalot M, Henrissat B, Kües U, Lucas S, Van De Peer Y, Podila GK, Polle A, Pukkila PJ, Richardson PM, Rouzé P, Sanders IR, Stajich JE, Tunlid A, Tuskan G, Grigoriev I V. 2008. The genome of Laccaria bicolor provides insights into mycorrhizal symbiosis. Nature 452:88–92.

TABLE 1 Taxonomy of the genera representing the beech root-associated fungal community and the reference species chosen from the JGI MycoCosm database for mapping the RNA sequencing data

Phylum	Order	Genus	Species	Trophic mode	Guild[a]	JGI short name	JGI name	JGI Reference
Ascomycota	Helotiales	*Phialocephala*	*Phialocephala scopiformis*	symbiotroph	endophyte	Phisc1	Phialocephala scopiformis 5WS22E1 v1.0	(133)
Ascomycota	Helotiales	*Oidiodendron*	*Oidiodendron maius*	symbiotroph	ericoid mycorrhiza	Oidma1	Oidiodendron maius Zn v1.0	(134, 135)
Ascomycota	Helotiales	*Melioniomyces*	*Meliniomyces bicolor*	symbiotroph	ectomycorrhiza and ericoid mycorrhiza	Melbi2	Meliniomyces bicolor E v2.0	(135)
Ascomycota	Mytilinidales	*Cenococcum*	*Cenococcum geophilum*	symbiotroph	ectomycorrhiza	Cenge3	Cenococcum geophilum 1.58 v2.0	(82)
Basidiomycota	Agaricales	*Galerina*	*Galerina marginata*	saprotroph	saprotroph	Galma1	Galerina marginata v1.0	(136)
Basidiomycota	Agaricales	*Mycena*	*Mycena galopus*	saprotroph	leaf litter decomposer	Mycgal1	Mycena galopus ATCC-62051 v1.0	(137)
Basidiomycota	Agaricales	*Amanita*	*Amanita muscaria*	symbiotroph	ectomycorrhiza	Amamu1	Amanita muscaria Koide v1.0	(134)
Basidiomycota	Agaricales	*Amanita*	*Amanita rubescens*	symbiotroph	ectomycorrhiza	Amarub1	Amanita rubescens Přilba v1.0	(137)
Basidiomycota	Agaricales	*Cortinarius*	*Cortinarius glaucopus*	symbiotroph	ectomycorrhiza	Corgl3	Cortinarius glaucopus AT 2004 276 v2.0	(137)
Basidiomycota	Agaricales	*Laccaria*	*Laccaria amethystina*	symbiotroph	ectomycorrhiza	Lacam2	Laccaria amethystina LaAM-08-1 v2.0	(134)
Basidiomycota	Agaricales	*Laccaria*	*Laccaria bicolor*	symbiotroph	ectomycorrhiza	Lacbi2	Laccaria bicolor v2.0	(138)
Basidiomycota	Boletales	*Imleria*	*Imleria badia* syn: *Xerocomus badius*	symbiotroph	ectomycorrhiza (saprobic abilities)	Xerba1	Xerocomus badius 84.06 v1.0	(137)
Basidiomycota	Boletales	*Boletus*	*Boletus edulis*	symbiotroph	ectomycorrhiza	Boledp1	Boletus edulis Přilba v1.0	(137)

Basidiomycota	Boletales	*Scleroderma*	*Scleroderma citrinum*	symbiotroph	ectomycorrhiza	Sclci1	Scleroderma citrinum Foug A v1.0	(134)
Basidiomycota	Russulales	*Russula*	*Russula ochroleuca*	symbiotroph	ectomycorrhiza	Rusoch1	Russula ochroleuca Přilba v1.0	(137)
Basidiomycota	Russulales	*Lactarius*	*Lactarius quietus*	symbiotroph	ectomycorrhiza	Lacqui1	Lactarius quietus S23C v1.0	(137)
Basidiomycota	Thelephorales	*Thelephora*	*Thelephora terrestris*	symbiotroph	ectomycorrhiza	Theter1	Thelephora terrestris UH-Tt-Lm1 v1.0	(137)

[a]Guild: the type of known trophic mode at the species level (i.e., the species used as reference for mapping the RNA sequence read data).

TABLE 2 KEGG pathway enrichment analysis of the ectomycorrhizal fungi metatranscriptome[b]

Term	Term name	P adjusted
KEGG:01100	Metabolic pathways	5.3E-17
KEGG:01110	Biosynthesis of secondary metabolites	7.3E-11
KEGG:00230	Purine metabolism	8.1E-07
KEGG:01230	Biosynthesis of amino acids	9.4E-05
KEGG:01200	Carbon metabolism	1.3E-04
KEGG:00010	Glycolysis / Gluconeogenesis	2.5E-03
KEGG:00620	Pyruvate metabolism	5.9E-03
KEGG:00520	Amino sugar and nucleotide sugar metabolism	2.4E-02
KEGG:00030	Pentose phosphate pathway	2.5E-02
KEGG:00220	Arginine biosynthesis	2.9E-02
KEGG:00240	Pyrimidine metabolism	2.9E-02
KEGG:00680	Methane metabolism	6.3E-02
KEGG:00261	Monobactam biosynthesis	6.3E-02
KEGG:00250	Alanine, aspartate and glutamate metabolism	6.3E-02
KEGG:00910	Nitrogen metabolism	6.3E-02

[b]Enrichment analysis was performed in g:Profiler against the ascomycete *Aspergillus oryzae* (version e100_eg47_p14_7733820; date: 10/20/2020) since the model organism *Laccaria bicolor* is not available in g:Profiler. Terms indicate the KEGG pathways to which EC numbers are mapped; Term name indicates the KEGG pathways; P adjusted is the FDR corrected p value.

1104 **TABLE 3** Biomass and root and soil chemistry in control and ^{15}N-ammonium or ^{15}N-nitrate treated cosms[c]

Variable	Control	Ammonium	Nitrate	F value	P value
Biomass of CR (g $cosm^{-1}$)	3.44 ± 1.37 a	2.87 ± 1.21 a	3.40 ± 1.16 a	0.5395	0.5905
Biomass of FR (g $cosm^{-1}$)	0.88 ± 0.47 a	0.66 ± 0.41 a	0.70 ± 0.28 a	0.6865	0.5138
Biomass of EMF_RA (g $cosm^{-1}$)	0.32 ± 0.17 a	0.23 ± 0.04 a	0.20 ± 0.08 a	0.0759	0.9275
Soil dry mass (g $cosm^{-1}$)	1227 ± 202 a	1149 ± 310 a	1155 ± 466 a	0.141	0.8693
^{15}N enrichment (mg g^{-1} CR)	na	**0.11 ± 0.03 b**	**0.06 ± 0.02 a**	**9.8675**	**0.008512**
^{15}N enrichment (mg g^{-1} FR)	na	0.27± 0.11 a	0.21 ± 0.04 a	1.1993	0.295
^{15}N enrichment (mg g^{-1} EMRT)	na	0.64 ± 0.45 a	0.52 ± 0.11 a	0.0285	0.8768
^{15}N enrichment (mg g^{-1} soil)	na	0.0171 ± 0.0062 a	0.0237 ± 0.017 a	0.8583	0.3725
^{15}N enrichment in roots (mg $cosm^{-1}$)	na	0.53 ± 0.25 a	0.42 ± 0.22 a	0.7395	0.4067
^{15}N enrichment in soil (mg $cosm^{-1}$)	na	18.35 ± 4.63 a	20.76 ± 6.38 a	0.6558	0.4338
N (mg g^{-1} CR)	9.16 ± 2.28 a	10.48 ± 2.29 a	9.19 ± 1.77 a	0.9419	0.4065
N (mg g^{-1} FR)	**12.90 ± 1.72 a**	**14.68 ± 1.60 ab**	**15.13 ± 1.36 b**	**4.5612**	**0.02334**
N (mg g^{-1} EMRT)	16.07 ± 4.83 a	17.44 ± 0.06 a	18.69 ± 1.85 a	0.4571	0.6507
N (mg g^{-1} soil)	4.34 ± 3.06 a	3.98 ± 2.93 a	4.61 ± 3.85 a	4e-04	0.9996
C (mg g^{-1} CR)	**450.95 ± 5.74 ab**	**456.03 ± 8.04 b**	**444.97 ± 7.16 a**	**4.4774**	**0.02472**
C (mg g^{-1}FR)	479.61 ± 14.80 a	472.13 ± 21.32 a	467.36 ± 13.35 a	1.1062	0.3502
C (mg g^{-1} EMRT)	435.74 ± 93.60 a	462.10 ± 1.65 a	465.03 ± 9.07 a	0.202	0.8217
C (mg g^{-1} soil)	114.99 ± 88.14 a	104.78 ± 82.78 a	123.77 ± 113.81 a	0.0699	9.9327
C:N ratio in CR	51.93 ± 12.41 a	45.32 ± 10.40 a	50.00 ± 9.54 a	0.7282	0.4951
C:N ratio in FR	**37.70 ± 4.75 b**	**32.38 ± 2.43 a**	**31.05 ± 2.20 a**	**7.8149**	**0.003106**
C:N ratio in EMRT	28.12 ± 6.45 a	26.54 ± 0.00 a	25.02 ± 2.05 a	0.3095	0.7434
C:N ratio in soil	25.75 ± 2.90 a	25.78 ± 2.21 a	25.42 ± 2.75 a	0.0423	0.9586

$N\text{-}NH_4^+$ (mg g^{-1} FR)	0.11 ± 0.03 a	0.09 ± 0.03 a	0.09 ± 0.03 a	0.3329	0.7253
$N\text{-}NO_3^-$ (mg g^{-1} FR)	1.96 ± 0.32 a	2.59 ± 0.73 a	1.87 ± 0.46 a	2.2306	0.1634
Glucose (mg g^{-1} FR)	16.99 ± 2.73 a	16.32 ± 2.20 a	16.36 ± 1.98 a	0.1062	0.9003
Fructose (mg g^{-1} FR)	9.06 ± 1.23 a	8.51 ± 1.84 a	7.71 ± 0.90 a	0.9712	0.415
Sucrose (mg g^{-1} FR)	0.61 ± 0.47 a	0.51 ± 1.02 a	0.82 ± 1.64 a	0.0759	0.9275
Starch (mg g^{-1} FR)	21.20 ± 11.95 a	18.40 ± 8.66 a	16.03 ± 5.20 a	0.2411	0.7907
TNSC (mg g^{-1} FR)	47.87 ± 14.25 a	43.75 ± 12.51 a	40.93 ± 6.33 a	0.3484	0.7149

[c]Analyses were conducted two days after watering each cosm with 35 mg ^{15}N. Mean soil pH was 3.6 ± 0.1 and mean relative soil water content was 47.6 ± 28.9% (n = 25) across all studied cosms. Data in table shows means ± SD for dry samples. For dry mass: control (n = 9), ammonium (n = 8), nitrate (n = 8). For ^{15}N, C and N: control (n = 9), ammonium (n = 7), nitrate (n = 7), except for root tips where control (n = 5), ammonium (n = 2), nitrate (n = 3). For ammonium-N, nitrate-N and non-structural carbohydrates in FR, n = 4 per treatment. Significant differences among treatments (control, ammonium, nitrate) at $p < 0.05$ (Tukey HSD test) are shown in rows and marked in bold. Abbreviations: coarse roots (CR), fine roots (FR), ectomycorrhizal root tips (EMRTs), TNSC (total non-structural carbohydrates), na = not applicable because mean ^{15}N values of non-labeled controls were subtracted from the ^{15}N-treated samples.

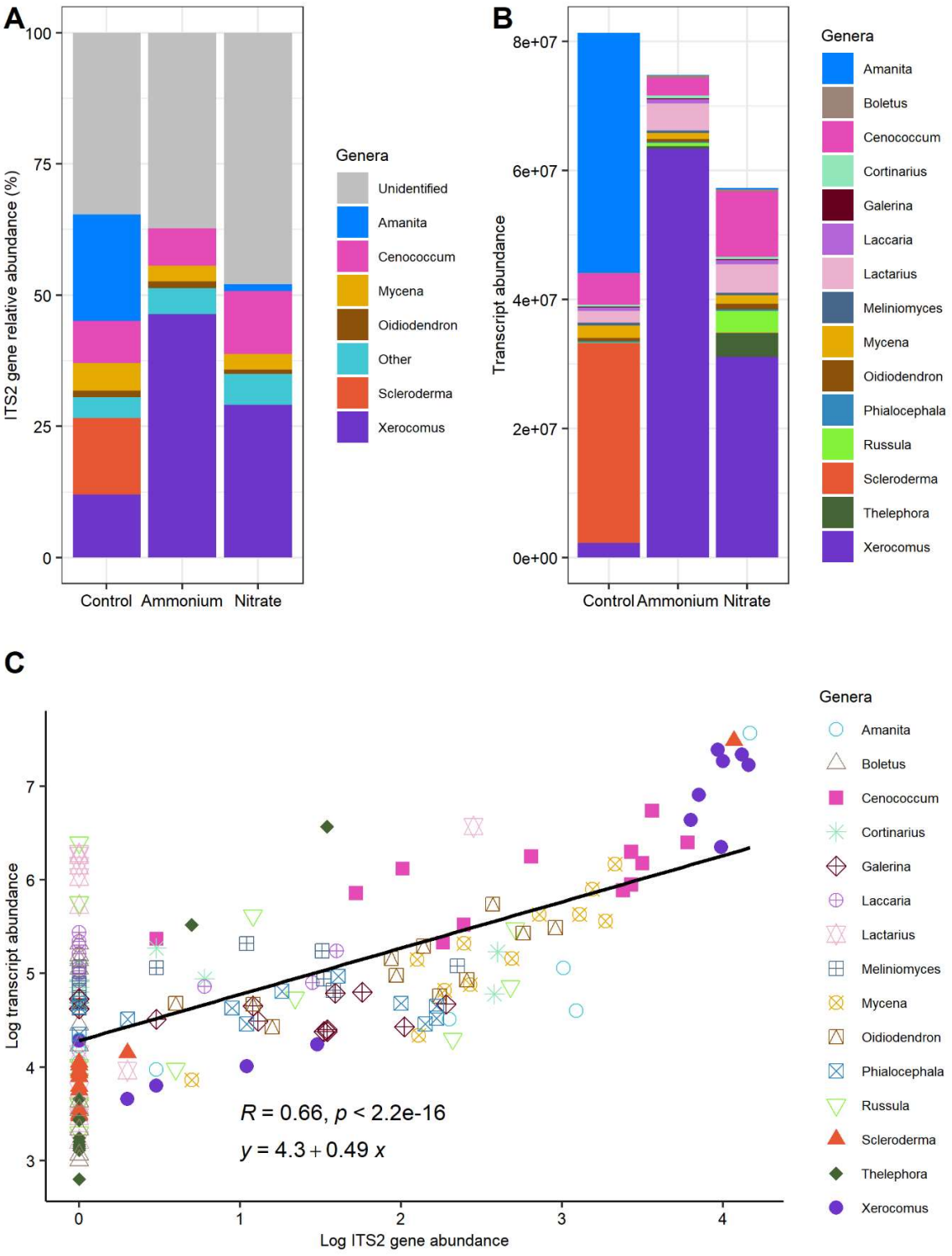

FIG 1 Relative abundance of root-associated (RAF) fungi based on ITS2 barcoding (A), raw counts of the metabolically active fungi based on RNA sequencing characterized by

taxonomy (B) and Pearson correlation between DNA-based and RNA-based abundances of the fungal genera (C). RAF were studied on roots of European beech (*Fagus sylvatica*) grown in native forest soil, treated with either water (control), ammonium or nitrate for two days before harvest, (n = 4 per treatment).

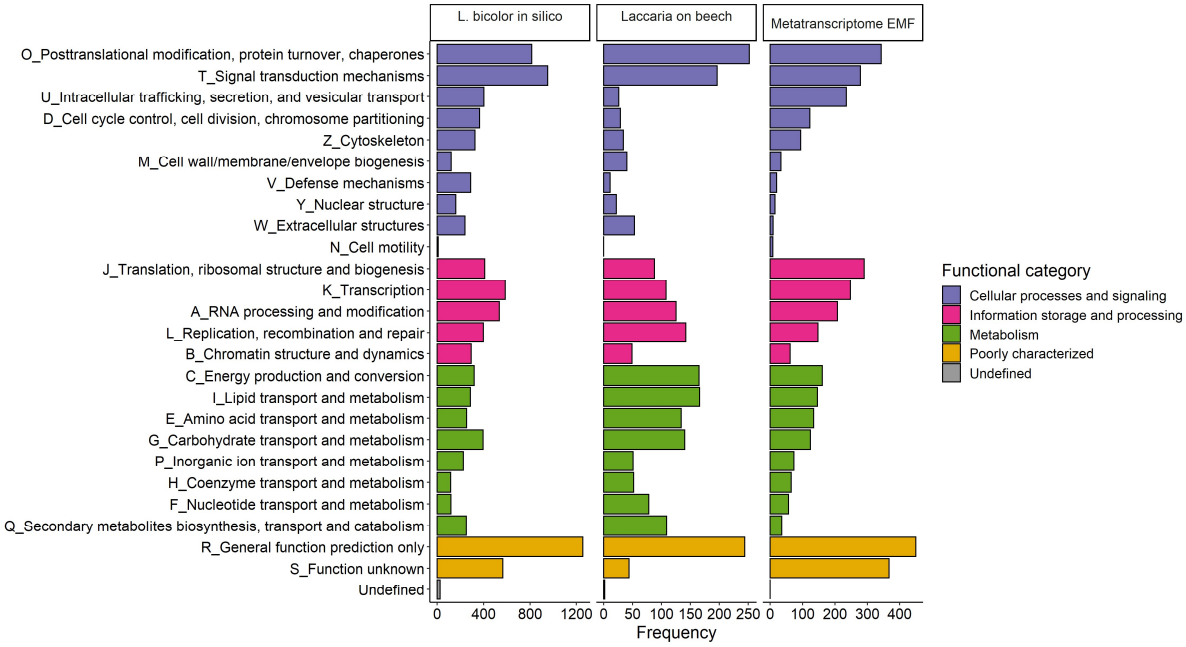

FIG 2. Functional classification of the ectomycorrhizal fungi (EMF) metatranscriptome according to KOG functional groups. The figure shows the distribution of KOG functions for the model ectomycorrhizal fungus *Laccaria bicolor* (*in silico* analyses of the published genome (138)), KOG functions in the transcriptome of the genus *Laccaria* in this experiment (*Laccaria* on beech), and in the entire ectomycorrhizal fungal metatranscriptome in this experiment (Metatranscriptome EMF).

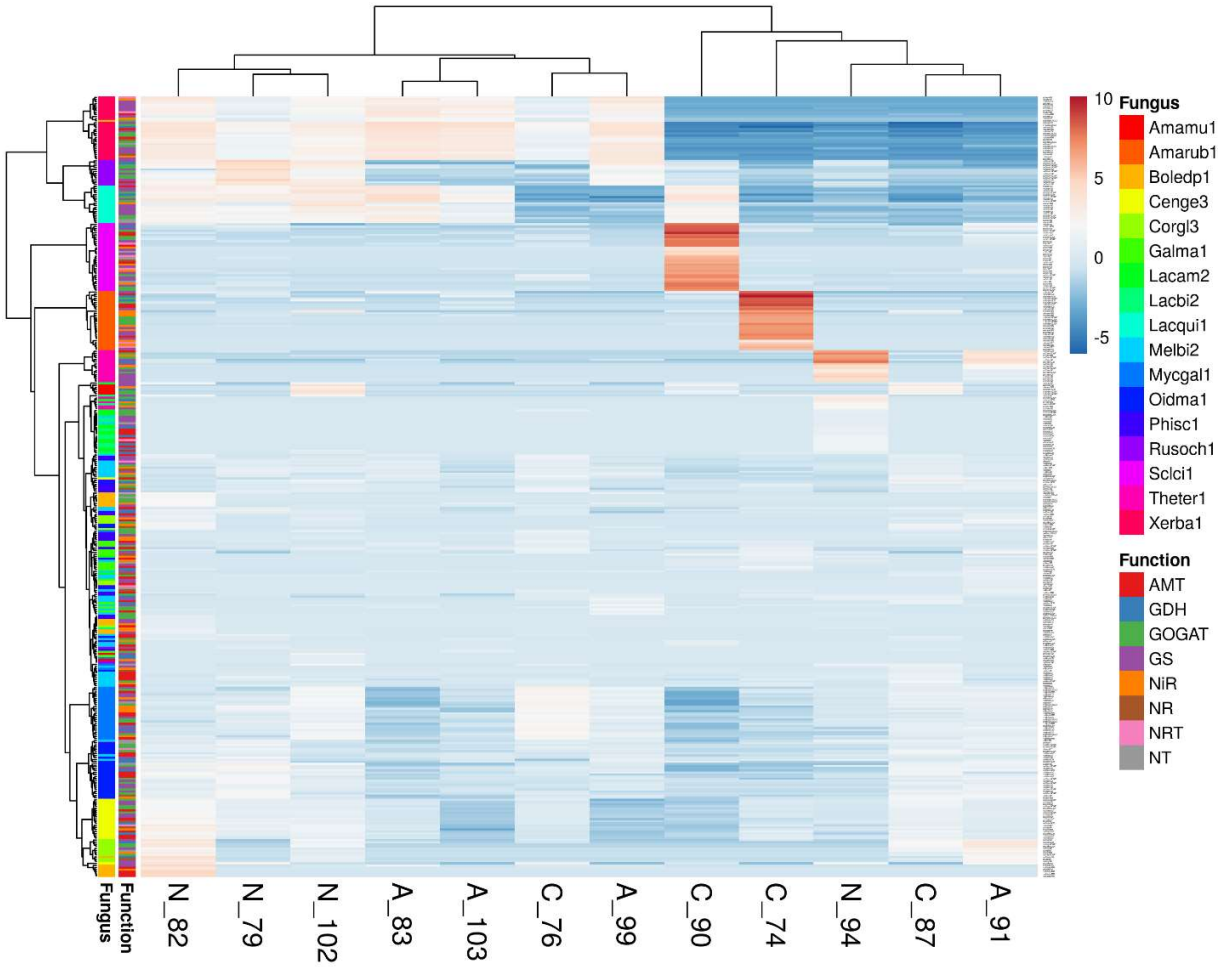

FIG 3: Cluster analysis of N-related transporters and enzymes represented by transcript abundances for ectomycorrhizal, endophytic and saprotrophic fungi colonizing beech roots. C = control, A = ammonium treatment, N = nitrate treatment, abbreviations for the fungi are shown in Table 1. Original values of the transcript levels were ln(x + 1)-transformed. Rows are centered; no scaling is applied to rows. Both rows and columns are clustered using Euclidean distance and Ward linkage. 369 rows, 12 columns.

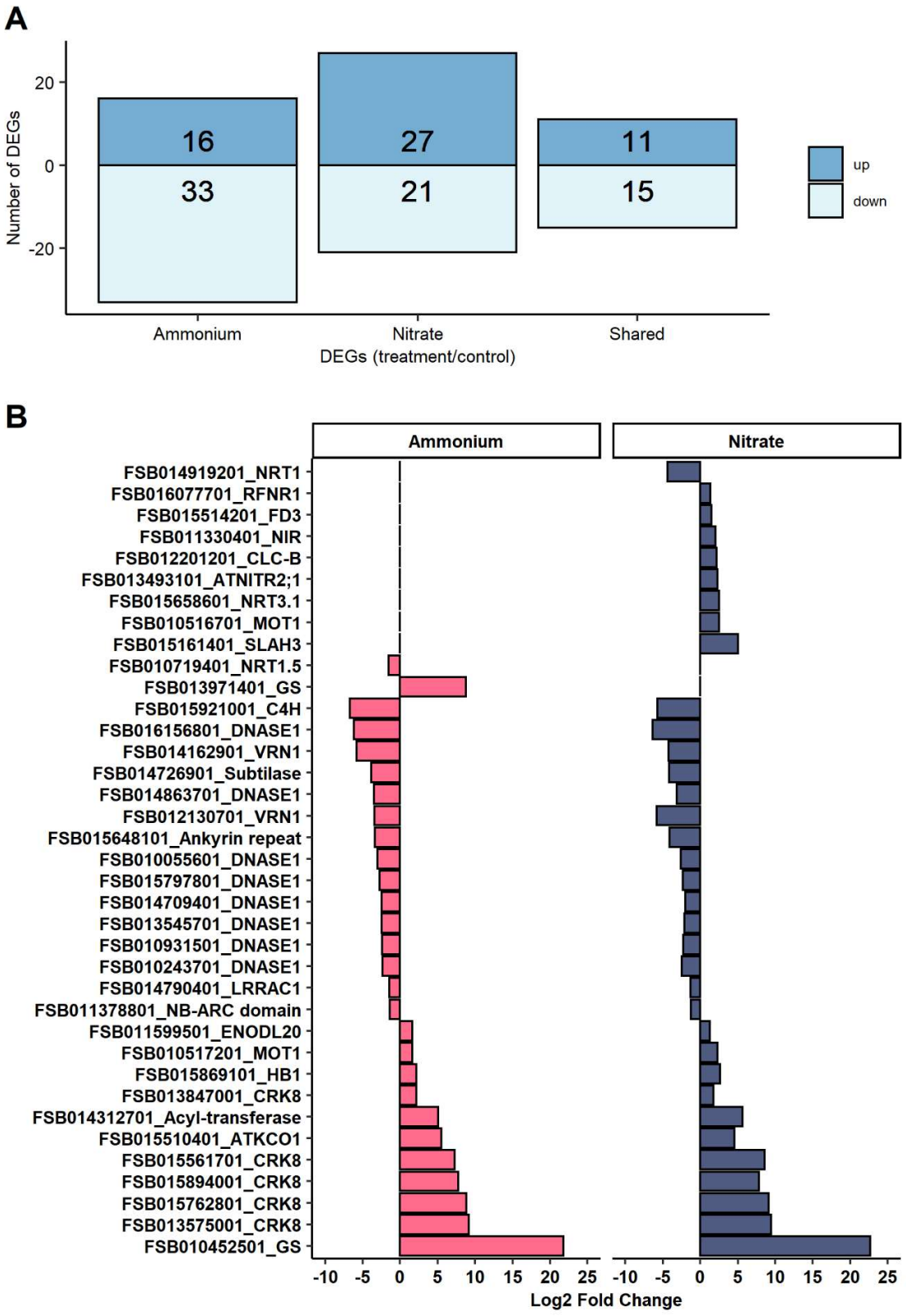

1135

1136 **FIG 4** Differentially expressed genes (DEGs) in response to ammonium or nitrate
1137 exposure. A) Number of unique and shared DEGs (padj < 0.05 and 2-fold change) in
1138 response to ammonium or nitrate treatment. B) Log2-fold changes of shared DEGs and
1139 DEGs related to N-metabolisms in beech roots in response to increased ammonium or
1140 nitrate treatment relative to control conditions (n = 4 per treatment). The complete
1141 information, gene model ID and names are provided in Data set 5.

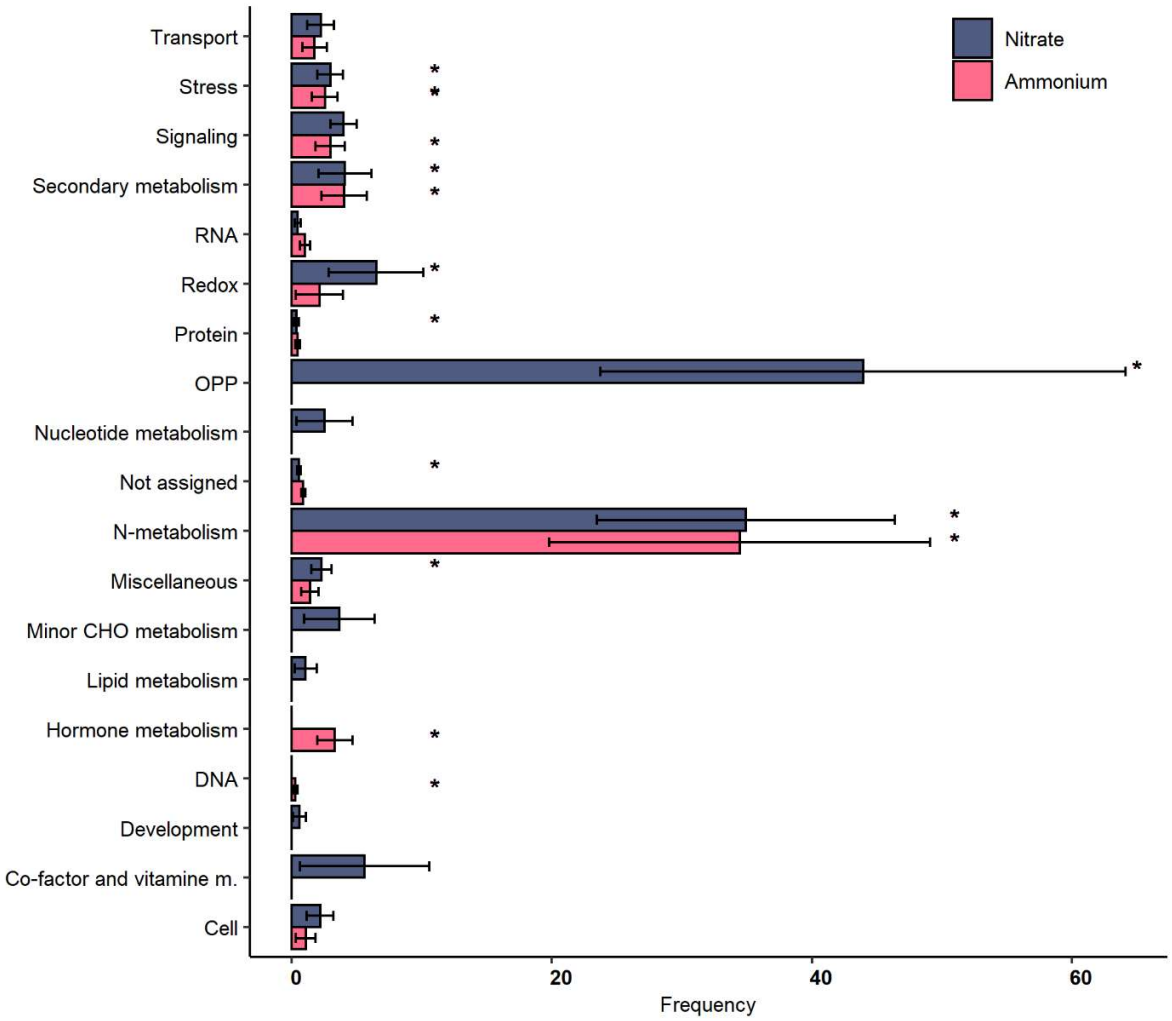

1142

1143 **FIG 5** Classification of beech root DEGs in response to nitrate or ammonium treatment.

1144 Genes were classified according to Mapman bins using Classification superviewer in

1145 BAR (http://bar.utoronto.ca/ntools/cgi-bin/ntools_classification_superviewer.cgi). Bins

1146 that were statistically significantly enriched are marked by an asterisk.

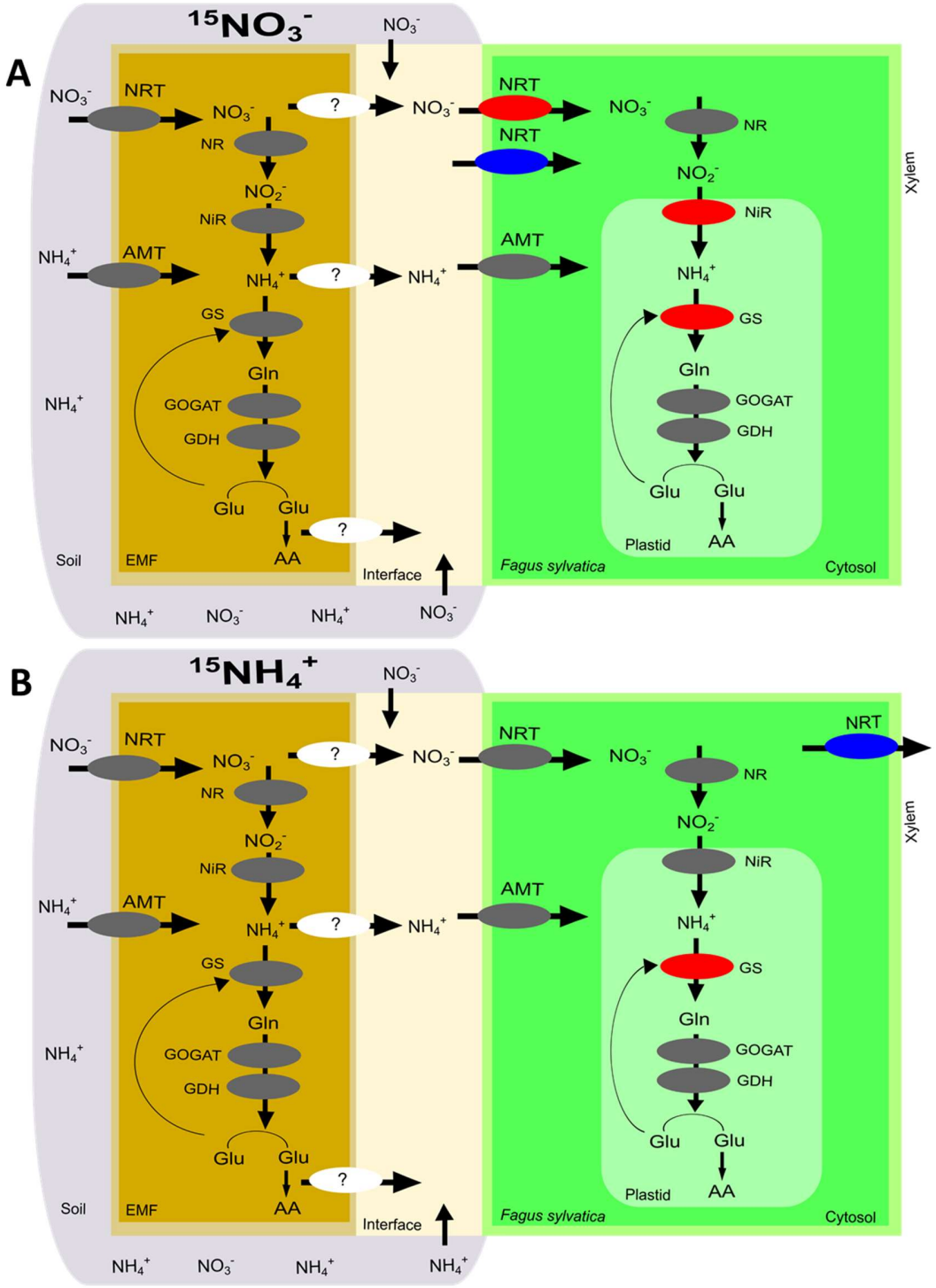

FIG 6 Scheme of the pathway for N uptake and assimilation in EMF and *Fagus sylvatica* based on transcription profiles. Regulation of ectomycorrhizal fungi and host transcripts encoding for transporters and enzymes involved in N uptake and assimilation detected

in the nitrate treatment (A) and in the ammonium treatment (B). NRT: nitrate/nitrite transporter, NR: nitrate reductase, NiR: nitrite reductase; AMT: ammonium transporter, GS: glutamine synthetase, GOGAT: glutamate synthase; GDH: glutamate dehydrogenase. Gray: detected but not regulated, Red: upregulated, Blue: downregulated, White: not detected.